TEMPORAL CHANGES OF THE MICROCIRCULATORY-MITOCHONDRIAL FUNCTIONS IN EXPERIMENTAL RODENT SEPSIS

Ph.D. Thesis

Roland Fejes MD

Supervisor: Szabolcs Péter Tallósy Ph.D.

Institute for Surgical Research
Doctoral School of Multidisciplinary Medical Sciences
Albert Szent-Györgyi Medical School
University of Szeged

Szeged

2024

TABLE OF CONTENTS

List of abbreviations **5**
Summary **6**
1.1. Definitions of sepsis 7
1.2. Immunopathophysiology of sepsis 8
1.3. Preclinical modeling of sepsis 8
1.4. Macrocirculation and oxygen dynamics 9
1.5. Microcirculation 9
1.6. Mitochondrial functions and metabolic processes 10
1.7. The concept of microcirculatory and mitochondrial distress 11
2. Main goals **12**
3. Materials and methods **13**
3.1. Ethical permissions and animals used in the experiments 13
3.2. Aims, protocol, and main results of the preliminary study 14
3.3. Microbial characterization of the fecal inoculum 15
3.4. Experimental protocol in Study 1 16
3.5. Experimental protocol in Study 2 16
3.6. Anesthesia, surgical preparation, and invasive cardiopulmonary monitoring 17
3.7. Measurement of serum markers; assessment of ROFA score 18
3.8. Examination of ileal microcirculation with Incident Dark Field imaging 18
3.9. Assessment of hepatic mitochondrial functions with high-resolution respirometry 19
3.10. Statistical analysis 20
4. Results **21**
4.1. Study 1 21
4.1.1. Animal well-being; mortality 21
4.1.2. Global and subcellular oxygen dynamics; inflammatory markers 22
4.1.3. Changes in ROFA score 23
4.1.4. Microbial background of the fecal inoculum and the ascites 24
4.1.5. Association between the inducing bacterial dose and the severity of organ failure 26
4.1.6. ROFA score components at 24h after mono- and polymicrobial inocula 27
4.2. Study 2 29
4.2.1. Animal well-being and mortality 29
4.2.2. Changes in inflammatory and multi-organ failure markers 29
4.2.3. Changes in macrohemodynamics 30

4.2.4. Changes in oxygen dynamics 31
4.2.5. Changes in microhemodynamics 32
4.2.6. Changes in liver mitochondrial functions 33
4.2.7. Receiver operating characteristic (ROC) curve analyses 34
4.2.8. Correlation between mitochondrial and microcirculatory parameters and the ROFA score 35
4.2.9. Correlation between mitochondrial and microcirculatory parameters 36
5. Discussion 37
5.1. The impact of the microbial composition of inocula on sepsis progression 37
5.2. Temporal changes in the composition of the bacterial content during sepsis progression 38
5.3. The possible contribution of microcirculatory and mitochondrial changes to the severity of organ dysfunction in experimental sepsis 39
5.4. Limitations 44
6. New findings 45
7. Funding 45
8. Acknowledgements 46
9. References 47
Disclosures 56
ANNEXES 57

List of publications

List of publications related to the Ph.D. thesis (IF: 9.59)

I. Szabolcs Péter Tallósy, Marietta Zita Poles, Attila Rutai, Roland Fejes, László Juhász, Katalin Burián, József Sóki, Andrea Szabó, Mihály Boros, József Kaszaki. **The microbial composition of the initial insult can predict the prognosis of experimental sepsis**. *Scientific Reports*, 2021; 11(1):22772. **IF: 4.9; D1**

II. Roland Fejes, Attila Rutai, László Juhász, Marietta Zita Poles, Andrea Szabó, Mihály Boros, József Kaszaki, Szabolcs Péter Tallósy. **Microcirculation-driven Mitochondrion Dysfunction during the Progression of Experimental Sepsis.** *Scientific Reports*, 2024;14: 7153. **IF: 4.6; D1**

List of publications not included in the Ph.D. thesis (IF: 13.93)

I. Attila Rutai,* Roland Fejes,* László Juhász, Szabolcs Péter Tallósy, Marietta Zita Poles, Imre Földesi, András Tamás Mészáros, Andrea Szabó, Mihály Boros, József Kaszaki. **Endothelin A and B Receptors: Potential Targets for Microcirculatory-Mitochondrial Therapy in Experimental Sepsis.** *Shock*, 2020; 54(1): 87–95. (*equal contribution) **IF: 2.55; Q1**

II. László Juhász, Attila Rutai, Roland Fejes, Szabolcs Péter Tallósy, Marietta Zita Poles, Andrea Szabó, Imre Szatmári, Ferenc Fülöp, László Vécsei, Mihály Boros, József Kaszaki. **Divergent Effects of the N-Methyl-D-Aspartate Receptor Antagonist Kynurenic Acid and the Synthetic Analog SZR-72 on Microcirculatory and Mitochondrial Dysfunction in Experimental Sepsis.** *Frontiers in Medicine*, 2020; 7:566582. **IF: 5.09; Q1**

III. Attila Rutai, Bettina Zsikai, Szabolcs Péter Tallósy, Dániel Érces, Lajos Bizánc, László Juhász, Marietta Zita Poles, József Sóki, Zain Baaity, Roland Fejes, Gabriella Varga, Imre Földesi, Katalin Burián, Andrea Szabó, Mihály Boros, József Kaszaki. **A Porcine Sepsis Model with Numerical Scoring for Early Prediction of Severity.** *Frontiers in Medicine*, 2022; 9:867796. **IF: 5.09; Q1**

IV. Roland Fejes, Tamás Szűcsborus, András Czombos, Csaba Góg, Zoltán Ruzsa. **Managing Patients with Overlapping High Risk for Bleeding and Thromboembolic Events.** *Cureus Journal of Medical Science*, 2024; 16(2):e53557. **IF: 1.2**

V. Fejes Roland,* Kovács-Huber Róbert,* Góg Csaba, Kádár Csilla. **Intenzív Inzulinkezelés Korai Deeszkalálásának Lehetőségei [Options for Early De-escalation of Intensive Insulin Treatment].** *Magyar Belorvosi Archívum*, 2024; 77: 45–48. (*equal contribution) **IF: 0**

List of abbreviations

ADP: adenosine diphosphate
ALT: alanine aminotransferase
AST: aspartate aminotransferase
ATP: adenosine triphosphate
AUC: area under the curve
CFU: colony-forming unit
CLP: cecum ligation and puncture
CO: cardiac output
CytC: cytochrome c
CytC%: cytochrome c control efficiency
DAMP: damage-associated molecular pattern
DO_2: oxygen delivery
ET-1: endothelin-1
ExO_2: oxygen extraction
FiO_2: fraction of inspired oxygen
Hb: hemoglobin
HR: heart rate
ICU: intensive care unit
IDF: incident dark field
IL-6: interleukin-6
ip: intraperitoneal
iv: intravenous
$LEAK_{Omy}$: oligomycin-induced leak respiration
MALDI-TOF MS: matrix-assisted laser desorption/ionization time-of-flight mass spectrometry
MAP: mean arterial pressure
MMD: microcirculatory-mitochondrial distress
MOF: multi-organ failure
MQTiPSS: Minimum Quality Thresholds in Pre-Clinical Sepsis Studies
mtOM: mitochondrial outer membrane
$mtVO_2$: mitochondrial oxygen consumption
MVH: microvascular heterogeneity
NO: nitric oxide
OxPhos: oxidative phosphorylation
PAMP: pathogen-associated molecular pattern
PaO_2: partial pressure of arterial oxygen
PPV: proportion of perfused vessels
RCR: respiratory control ratio
ROFA: rat-specific organ failure assessment
ROC: receiver operating characteristic
ROS: reactive oxygen species
RSS: rat-specific sickness score
SaO_2: oxygen saturation of the arterial blood
SvO_2: oxygen saturation of the venous blood
SIRS: systemic inflammatory response syndrome
SOFA: sequential organ failure assessment
VO_2: oxygen consumption

Summary

Sepsis is a life-threatening organ dysfunction caused by a dysregulated host response to infection. The pathophysiology is complex with unknown factors, but microcirculatory and mitochondrial distress (MMD) is considered a key factor in its progression. The investigation of sepsis pathophysiology is greatly limited by the lack of animal models reliably representing the human clinical course. The microbiological background is often unknown, and the causes of the mismatch between microhemodynamics and mitochondrial respiration are not well understood.

Our goals were to (1) study the time course of multi-organ failure (MOF) development in experimental peritonitis, (2) examine how the microbiological characteristics of the inducing inocula change in the peritoneal fluid in association with sepsis severity, and (3) track concurrent changes in splanchnic microcirculation and mitochondrial function to characterize their relationship and time dependence in Sprague Dawley rats.

In Study 1 we aimed to characterize the microbial background of a standardized intraabdominal sepsis, in Study 2 we focused on the relationships between MMD parameters. In both studies, sepsis was induced by intraperitoneal injection of pooled fecal inoculum, and the progression was assessed using a Rat-Specific Sickness Score (RSS). After predetermined periods (12, 24, 48, or 72h in Study 1, and 12, 16, 20, 24, and 28h in Study 2, respectively), the animals were anesthetized for cardiopulmonary monitoring, sampling for mitochondrial examinations (using high-resolution respirometry) and assessing MOF severity with a Rat-specific Organ Failure Assessment (ROFA) score. Blood samples were collected to measure inflammatory and organ function markers, while ileal microcirculatory measurements were performed using Incident Dark Field imaging.

In Study 1, animal well-being (RSS), organ function (ROFA), and inflammatory parameters (interleukin-6 and endothelin-1 levels) changed significantly between 24h and 48h after fecal inoculation. A retrospective evaluation of the induction inoculum proved that the nature of the inoculum (monoculture or polymicrobial) significantly affects the outcome, as the mortality rate peaked at 24h in animals injected with E. coli monocultures. In Study 2, the most severe microcirculatory disturbances (decreased microperfusion with increased heterogeneity) were observed at 16h; however, the deterioration in the mitochondrial oxidative phosphorylation (OxPhos) and a parallel increase in mitochondrial outer membrane damage developed later, at 20h after sepsis induction. The intestinal microvascular perfusion failure showed higher predictive value for septic MOF than those of hepatic mitochondrial functional changes.

These results show that the mono- or polymicrobial nature of the inoculum affects both the progression and mortality of sepsis. Microcirculatory insufficiency after a septic event appears to be a primary issue, while the temporary loss of mitochondrial function likely reflects adaptive processes or suggests the presence of mitochondrial subpopulations with varying sensitivity to hypoxia.

1. Introduction

1.1. Definitions of sepsis

The term *sepsis* was first used in a medical context to describe a dangerous, odoriferous, biological decay of the body (Salomão et al. 2019). Sepsis is not a clearly definable disease, and, despite advances in medical science, it remains difficult to diagnose and treat effectively (Trásy and Molnár 2023). The modern conception dates back to the 1980s (Bone et al. 1987), when the condition was identified as "sepsis syndrome," and later as a specific clinical entity (Bone et al. 1989). In 1991, the Sepsis-1 consensus was established in response to the growing need among clinicians, using the systemic inflammatory response syndrome (SIRS) definition, which was based on measurable changes in inflammatory response (Bone et al. 1992). The Sepsis-2 definition in 2001 still followed this notion, although it was already emphasized that the pathogenesis encompasses a continuum of ongoing processes from sepsis to severe sepsis and septic shock (Dellinger et al. 2014). The latest nomenclature of the Sepsis-3 consensus recognized the inaccuracies and limited clinical utility of earlier definitions. Today sepsis is defined as life-threatening organ dysfunction caused by a dysregulated host response to infection (Singer et al. 2016). The introduction of the Sequential Organ Failure Assessment (SOFA) system has shifted clinical practice towards a more MOF-focused approach, as a condition with a suspected or documented infection and an acute increase of ≥ 2 SOFA points. Septic shock is a severe form of sepsis characterized by persistent hypotension requiring vasopressor therapy and elevated lactate levels despite adequate volume resuscitation. The characteristics of sepsis definitions over time and SIRS criteria are illustrated in Figure 1.

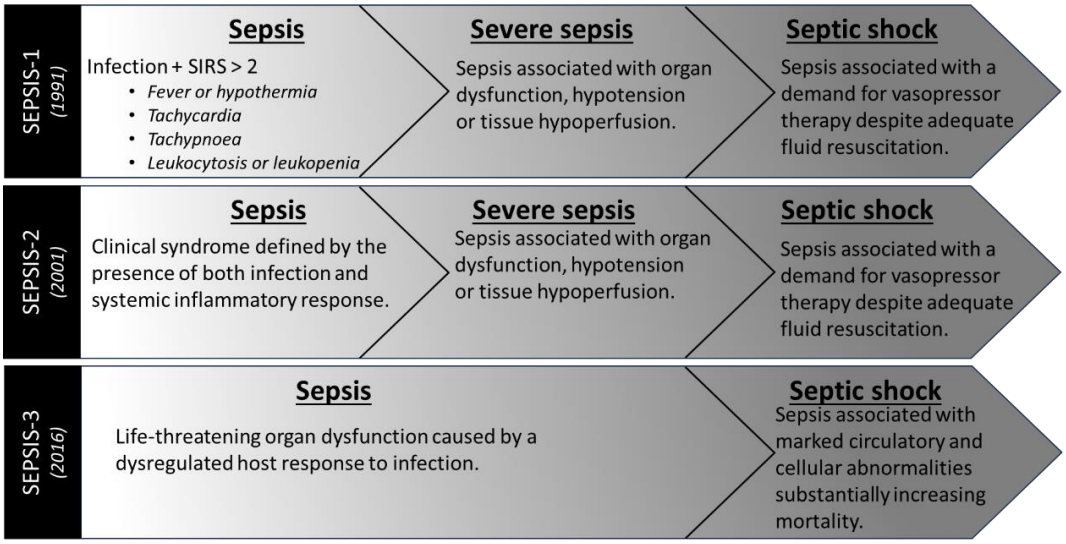

Figure 1. Evolution of sepsis definitions with their major characteristics.

1.2. Immunopathophysiology of sepsis

According to the original "germ theory" of sepsis, the inflammatory response is triggered by antigens originating from microbiological sources (later termed pathogen-associated molecular patterns, PAMPs; e.g., pathogen deoxyribonucleic and ribonucleic acids, lipopolysaccharides) (Cabrera-Perez et al. 2017). Furthermore, tissue damage-associated factors (also known as damage-associated molecular patterns, DAMPs) released from cells either through inflammasome activation or cell damage/death (e.g., cellular or mitochondrial deoxyribonucleic acid, ribonucleic acids, cytochrome c, and heat shock proteins) have also been identified as activators of the immune system (Wiersinga et al. 2014; Bianchi 2007). Innate immunity operates through various pattern recognition receptors, triggering a cascade of immune responses (Lewis et al. 2016). The activated immunoreaction causes the cleavage of proinflammatory cytokines, such as interleukin-1β (IL-1β) and IL-18 (Lamkanfi and Dixit 2014). During this response, various cell types are activated, leading to intracellular signaling pathways and activation of key transcription factors, such as nuclear factor kappa B and activator protein-1 (Arina and Singer 2021). Hence, sepsis has a complex pathobiology, involving several organ systems simultaneously, typically remote from the initial infection site (Nakamori et al. 2021). Traditionally, sepsis has been depicted as a biphasic model, with an early hyperinflammatory cytokine storm followed by a later immune paralysis (Liu et al. 2022). However, clinical evidence does not support sharply defined phases. Instead, sepsis is better understood as a dynamic condition where hyperinflammation and immune paralysis coexist, resulting from persistent and competing pro- and anti-inflammatory pathways (Wiersinga and Poll 2022).

1.3. Preclinical modeling of sepsis

Experimental models can provide a basis for the development of potential therapeutics, but an effective laboratory strategy cannot always be transferred to clinical practice (Rutai et al. 2022; Cai et al. 2023). The most recent Minimum Quality Threshold in Preclinical Sepsis Studies (MQTiPSS) criteria outline a recommended scheme for rodent experimental sepsis and highlight the importance of consecutive evaluation of established signs of organ failure similar to the SOFA scoring systems in humans (Osuchowski et al. 2018). Nevertheless, the findings of preclinical laboratory studies are still difficult to compare, as the magnitude of bacterial load is challenging to standardize and the composition of the microbiome at the time of infection is usually unknown. The bacterial strains of human or rat stool are broadly representative of the principally polymicrobial flora of the distal colon, and, therefore, intraabdominal administration

of fecal matter is considered a good rodent model for human peritonitis-linked sepsis (Wildner 2019; Jackson et al. 2017). Among the many cecum-ligation and puncture (CLP) alternatives, fecal slurries and intraabdominal injections of fresh or stored solutions of fecal suspensions can reduce the inherent variance of invasive surgical procedures (Buras et al. 2005; Coopersmith et al. 2018). Nevertheless, the composition and activity of competing microbial communities may vary greatly even in precisely quantified fecal doses if concise qualitative information on the invading microorganisms is lacking (Nandi et al. 2020). The question of whether a dominant strain or certain strains will collectively determine the initial and overall severity of sepsis is not yet fully understood. Furthermore, it has been shown that stand-alone E. coli strains can lead to fulminant sepsis with high early mortality (Murando et al. 2019).

1.4. Macrocirculation and oxygen dynamics

Changes in macrohemodynamics and oxygen dynamics are strongly interrelated in sepsis (Scheeren and Ramsay 2019). Due to the hyperinflammatory reaction, a hypermetabolic state can be also observed which is associated with increased tissue and cellular oxygen consumption (VO_2) and oxygen extraction (ExO_2). Oxygen delivery (DO_2) is increased to meet the energy needs of the cells, and this initial phase of septic reaction is usually characterized by normal or high cardiac output (CO) and high heart rate (HR), associated with a fall in peripheral vascular resistance (PVR). This phase is defined as a hyperdynamic state and is marked by a compensated cardiopulmonary system (Taeb et al. 2017). Propagation of sepsis may lead to a condition referred to as low output syndrome or a hypodynamic state, involving a significantly decreased CO, elevated PVR, and persistent hypotension (Perret 1980). All intermediate situations can be observed within these extremes. The most widely known circulatory parameter is blood pressure, which is an important component but not a reliable indicator of circulatory performance and tissue perfusion, as hypotension is a late marker of critical hypoperfusion (Meng 2021). Eventually, the balance between DO_2 and VO_2 becomes disrupted, leading to a cellular energy deficit with MOF being manifested (Armstrong et al. 2017).

1.5. Microcirculation

The microcirculation is composed of the smallest vessels in the circulatory system (< 100 μm in diameter) that ensure and regulate the distribution of blood flow in tissues and also modulate inflammatory responses (Ince 2005). Endothelial cells also play an active role in this process, sensing metabolic and physical signals and regulating the tone of arteriolar smooth muscle cells by releasing vasoactive substances (e.g., nitric oxide [NO] or endothelin) (Aird 2004). The patency of the microcirculation is profoundly disrupted in sepsis partially due to the unevenly overexpressed inducible NO synthase, leading to an arteriovenous shunt mechanism

(Hernandez et al. 2013; Trzeciak et al. 2008; Ince and Sinaasappel 1999). Endothelial cell-related electrophysiological signal transduction pathways can also be impaired, leading to a loss of control over arteriolar smooth muscle cells (Lidington et al. 2003; Ince 2005). Due to the sepsis-induced inflammatory reaction, circulating neutrophils are activated and show increased aggregability and margination in the postcapillary venules. Activated leukocytes produce reactive oxygen species (ROS) and other inflammatory mediators that directly damage microcirculatory structures, including the endothelial glycocalyx (Tyagi et al. 2009; Miranda et al. 2015). Collectively, these mechanisms contribute to a reduction in the number of perfused capillaries. The decrease in functional capillary density leads to a greater distance for oxygen to diffuse to nearby parenchymal cells. It should be noted that systemic hemodynamic parameters do not strictly follow the progression of microcirculatory dysfunction. Furthermore, microcirculation has been proposed as a better predictor for the severity of MOF and mortality than macrocirculatory parameters and restoration of microcirculatory flow became an important therapeutic target (Donati et al. 2013; Edul et al. 2012).

1.6. Mitochondrial functions and metabolic processes

Adenosine triphosphate (ATP) synthesis through mitochondrial oxidative phosphorylation (OxPhos) is the backbone of cellular metabolism. In simple infectious conditions, systemic VO_2 and metabolic activity can increase even by 60% compared to the basal metabolism to meet the energy needs of immune processes (Kreymann et al. 1993). Conversely, septic ICU patients show a less-pronounced increase in the metabolic rate from baseline (< 30%) with only limited increases in VO_2 and energy expenditure (Soop et al. 2004). There may be many factors in the background of this observation, but the precise mechanism is still a matter of debate. Inadequate mitochondrial fission-fusion mechanisms and disturbed autophagy may negatively influence the mitochondrial volume of cells (Nedel et al. 2023). Oxidative and nitrosative stress-induced membrane damage causes the breakdown of electron-transport chain coupling and increased proton leak, thus initiating a self-sustaining process (Brand 2016; Szabó 2003; Jastroch et al. 2010). Another mechanism that modulates the interaction between mitochondrial ROS and mitochondrial dysfunction is mitochondrial permeability transition pore opening, which induces calcium overload, ATP depletion, and dissipation of the mitochondrial membrane potential. The disruption of the delicate balance between DO_2 and VO_2 can be observed even at this molecular level, which, according to our current understanding, represents the ultimate stage, the smallest level in the development of MOF (Preau et al. 2021).

1.7. The concept of microcirculatory and mitochondrial distress

Systemic hemodynamic and global oxygenation parameters may not follow the sepsis progression closely, and microcirculatory oxygen transport can become independent of macrohemodynamic variables (Donati et al. 2013). The concept of microcirculatory and mitochondrial distress (MMD) has been introduced to highlight the mutual effect of these fragile physiological compartments (Ince 2005; De Backer et al. 2013). Recently, algorithms that support microcirculatory DO_2 to maintain mitochondrial VO_2 have been in the focus of clinical and basic research (Spronk et al. 2004). It should also be added that increased CO and a higher metabolic rate with preserved capillary perfusion in vital organs are usually present during the acute hyperdynamic phase of sepsis (Clowes et al. 1974; Lang et al. 1984; Protti et al. 2006). The early mitochondrial reaction is tissue-dependent but, in most cases, is characterized by increased VO_2 and a shift to a catabolic state (Brand 2016; Szabó 2003; Jastroch et al. 2010). Subsequently, a plateau is reached and the hypodynamic phase involves reduced cardiac performance, while tissue hypoperfusion is accompanied by hyperlacticemia and other signs of functional and structural mitochondrial damage (Kreymann et al. 1993). In this simplified outline, tissue mitochondria together with their supplier microcirculatory network are both major drivers of MOF (Rutai et al. 2020; Juhász et al. 2020; Fejes et al. 2024). However, it remains an open question whether these changes are causally related and, if so, how this bidirectional connection develops in time. Indeed, there are three possibilities for mitochondrial dysfunction: it may be a direct and early consequence of microcirculatory failure, thus being the promoter of progression; it can occur in parallel with microcirculatory events, interacting continuously and influencing the outcome jointly; or, in theory, it can occur independently. It is challenging to demonstrate causal links between the two arms of MMD even under standardized experimental conditions due to the web of connections and cross-reactions. Of note, microcirculatory and mitochondrial changes have not been investigated simultaneously in human sepsis in the pre- and post-MOF periods (Preau et al. 2021; Merz et al. 2020).

2. Main goals

1. Given the importance of a prolonged duration of clinical sepsis, we aimed to investigate the appropriate temporal characteristics of a standardized fecal inoculum-induced sepsis (6–72h) in terms of animal well-being and the development of organ dysfunction.
2. As the severity of sepsis may vary between individuals (including rats), we hypothesized that the bacterial composition within the fecal mass that initiates the insults could be an extremely important confounding factor and a decisive descriptor of the course of a septic scenario. Therefore, we retrospectively investigated how the microbiological parameters (bacterial count and composition) of the sepsis-inducing fecal inoculum influences the severity of intraabdominal sepsis.
3. Our third objective was to determine how the composition and germ count of the bacterial population change in the abdominal cavity as a function of time and how these factors influence sepsis severity.
4. Since recent literature suggests a link between sepsis-induced microcirculatory and mitochondrial dysfunction and clinical outcomes, we aimed to investigate the effects of these pathophysiological components on sepsis severity. Additionally, we aimed to simultaneously monitor the splanchnic microvascular status and concurrent mitochondrial function and to characterize their relationship and time dependency in our intra-abdominal sepsis model.

3. Materials and methods

Sepsis was induced by intraperitoneal (ip) injection of an inoculum prepared from rat feces. In Study 1, our primary objective was to optimize the model in which the course of organ dysfunction associated with the septic process can be characterized. During the first phase, we wanted to find the optimal germ count which induces sepsis of appropriate severity without causing a fulminant reaction. As a sufficiently high and standard germ count was needed, an incubation process was mandatory. Therefore, in preliminary studies, we also examined the effects of filtration and incubation on the microbial characteristics of the inoculum. Based on the results of these preliminary experiments, we were able to use an inoculum with a relatively narrowed microbial concentration range in further studies. Since the severity of sepsis was more pronounced in certain animals, we also retrospectively investigated how the qualitative characteristics of the inoculum influenced the outcome of sepsis. In Study 2, we used a similar experimental design but focused on the correlations between parameters describing microcirculatory and mitochondrial function and how these correlate with sepsis severity or predict its outcome. The main experimental methods in the different studies are shown in Table 1.

Table 1. Experimental methods in the protocols

	Preliminary study	Study 1	Study 2
Quantitative microbiological assessment	+	+	
Qualitative microbiological assessment	+	+	
Well-being–related sickness score	+	+	+
Organ failure assessment score		+	+
Microcirculatory measurements			+
Mitochondrial measurements		+	+

3.1. Ethical permissions and animals used in the experiments

Procedures were performed following the National Institutes of Health Guide for the Care and Use of Laboratory Animals (NIH Publication No. 85-23, Revised 1996) and EU and national Hungarian directives (2010/63/EU and Government Decree 40/2013/Korm, respectively) for the protection of animals used for scientific purposes. The study was approved by the University of Szeged Animal Welfare Committee and the National Scientific and Ethical Committee, the national competent authority in Hungary (ETT-TUKEB; license number: V/175/2018).

Male Sprague Dawley rats were used that had previously been housed in plastic cages within a temperature-controlled room (21–23°C) with a daily 12/12h light and dark cycle. They had unrestricted access to standard rodent chow and water.

3.2. Aims, protocol, and main results of the preliminary study

We aimed to induce peritoneal sepsis with injections of standardized bacterial counts within a defined range but without limiting the variability in the microbiome composition. Therefore, we ran a preliminary study aiming **(1)** to clarify the effects of filtration on the inocula, **(2)** to determine the optimal germ count in the inducing inocula confirmed with a prognosis analysis, and **(3)** to optimize the duration of the incubation. The experimental protocol, including the fecal inoculum preparation, is shown in Figure 1.

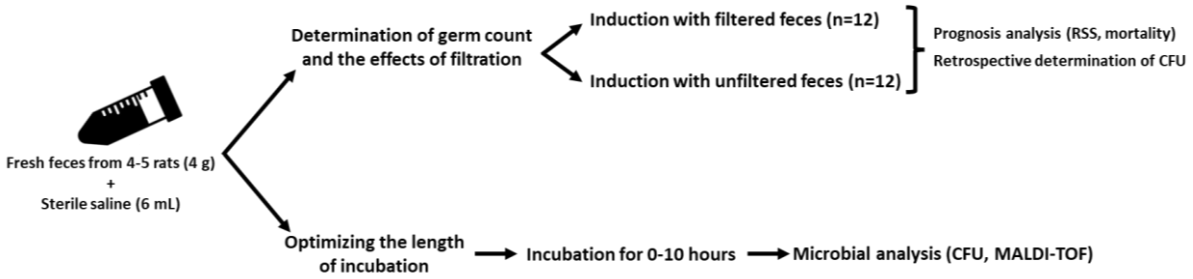

Figure 1. Experimental protocol in the preliminary study. Fresh feces (~ 4 g) was randomly collected from age- and body weight-matched healthy rats (n = 4–5). The fecal mass was mixed with 6 mL saline in sterile 10 mL Falcon tubes, vortexed, and diluted 3:1. The resulting inoculum was then divided into two equal amounts. As the first aim was to determine the germ count and the effects of filtration, a group of animals received different doses of the fecal inducer suspension (3–6 mL kg^{-1}) with or without filtration (n = 12, respectively) to test the relationship between germ count and mortality rate. A rat-specific sickness score (RSS) was used to assess the general condition of the animals and their potential need for a humane endpoint. The remaining inocula were subjected to colony-forming unit (CFU) determination, providing detailed retrospective information on the bacterial count used in the induction. The other half of the fecal mass remaining from the first split was incubated for 10h at 37°C. The diversity of bacterial strains in the suspension was examined every hour using matrix-assisted laser desorption/ionization time-of-flight mass spectrometry (MALDI-TOF MS) in the same stock suspension of fecal inoculum.

The general well-being of the animals was assessed using a 0–9-point rat-specific sickness scoring (RSS) system (Table 2), where a cumulative value above 6 was considered a humane endpoint for euthanasia. There was no significantly elevated RSS value and mortality below 1.02×10^6 colony-forming units (CFU) (see method in Section 3.3), and no significant changes occurred in the sickness score for 24h (see Figure 1b in Tallósy et al. 2021). However, microbial concentration above 5.6×10^6 CFUs resulted in a high mortality rate (> 90%) in the first 12–16h. Therefore, bacterial content between 1.02×10^6 and 5.6×10^6 CFUs was administered to investigate sepsis-associated organ dysfunctions and changes in Study 1 and Study 2.

In addition, the influence of filtration was also examined in the context of mortality. We found that mortality was independent of the germ count when induction was performed without filtration (see Supplementary Material S1 in Tallósy et al. 2021). However, a higher germ count meant higher mortality with filtration due to the reduced random variability of fecal flocculants providing an adhesion surface for living microorganisms (see data in Supplementary Material S1 in Tallósy et al. 2021). The qualitative microbiological analysis (see method in Section 3.3) demonstrated a significant decrease in the number of bacterial strains after only 10h of incubation at 37°C because of the log phase of microbial competition for population growth (see data in Supplementary Material S2 in Tallósy et al. 2021).

Table 2. Assessment scheme of the condition of animals with rat sickness scores

RSS score	Condition of fur	Posture	Mobility	Alertness	Weight	Temperature
0	Not altered	Not altered	Not altered	Not altered	+0–10g	Not altered
1	Piloerection	Altered weight distribution	Slow/stiff movement	Decreased	–5–10g	Fever or hypothermia
2	–	Hunched back	No movement	No reaction	–20g	–

3.3. Microbial characterization of the fecal inoculum

0.1 mL samples of the inocula were used for microbiological analysis to determine CFU and identify the bacterial strains. CFU was determined using the standard pour-plate count method (Sanders 2012) and converted into the cell number per milliliter of the original inoculant (CFU mL^{-1}). Species-selective media and matrix-assisted laser desorption/ionization time-of-flight (MALDI-TOF) mass spectrometry (MS; Bruker Daltonics, Germany) was used to analyze the bacterial composition of the inoculum. Spectra were obtained from the microbiological samples with the Microfex LT system (Bruker Daltonik, Bremen, Germany) and analyzed with MALDI BIOTYPER 3.3 software (Bruker Daltonik, Bremen, Germany) (Nagy et al. 2012) for the MALDI-TOF analysis. The results of the bacterial composition were typically available 48h after the completion of the inoculum preparation procedure (Sauer et al. 2008; Idelevich et al. 2014).

3.4. Experimental protocol in Study 1

Sample size estimation was performed assuming approx. 20% mortality after 24h. If the presumed true hazard ratio of septic subjects relative to sham-operated animals is 0.2 with a power of $1 - \beta = 0.9$ and the Type I error probability is $\alpha = 0.05$, the inclusion of 12 septic and 12 sham-operated animals was recommended at each selected time point. The experimental protocol for Study 1 is shown in Figure 2.

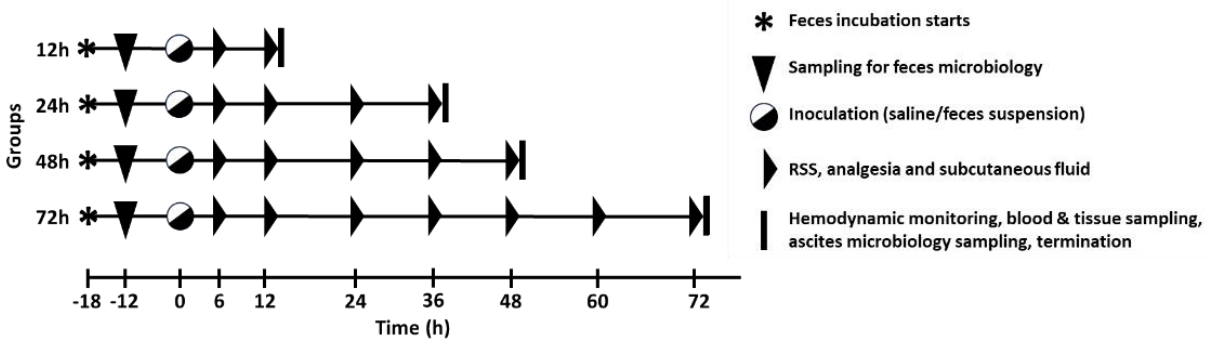

Figure 2. Experimental protocol and groups in Study 1. The animals (380 ± 30g in both groups) were randomly assigned to sham-operated ($n_{\Sigma} = 49$) and septic groups ($n_{\Sigma} = 51$), which were randomly further divided into four independent groups each (sham-operated: $n_{12h} = 13$, $n_{24h} = 12$, $n_{48h} = 12$, $n_{72h} = 12$; septic: $n_{12h} = 13$, $n_{24h} = 13$, $n_{48h} = 13$, $n_{72h} = 12$) according to a termination timeline set between 12 and 72h. Based on the data obtained in the preliminary study, the filtered inoculum was injected intraperitoneally (ip) using a 21G needle at a volume of 5 mL kg^{-1} at a dose range of 1.02×10^6–5.6×10^6 CFUs. The rats in the sham-operated groups received saline in the same volume. The general condition of the animals was evaluated at 6h after the ip injections and every 12h thereafter using the RSS scoring system. At time points of sickness assessment, the animals received 10 mL kg^{-1} crystalloid solution sc (Ringerfundin, B. Braun, Hungary) to avoid dehydration and 15 µg kg^{-1} buprenorphine sc (Bupaq, Merck, USA) to maintain analgesia. At the end of progression in each group, the animals were anesthetized, and hemodynamic monitoring (see Sections 3.6 and 3.7), blood and tissue sampling, and ascites sampling for microbiological measurements were performed (see Section 3.3). At the end of the protocol, all the animals were terminated.

3.5. Experimental protocol in Study 2

Sample size was estimated assuming approx. 20% mortality after 24h. If the presumed true hazard ratio of the septic subjects relative to the sham-operated animals was 0.2 with a power of $1 - \beta = 0.8$ and the Type I error probability was $\alpha = 0.05$, the inclusion of 8 septic and 8 sham-operated animals was recommended for each time point that had been selected. The experimental protocol for Study 2 is shown in Figure 3.

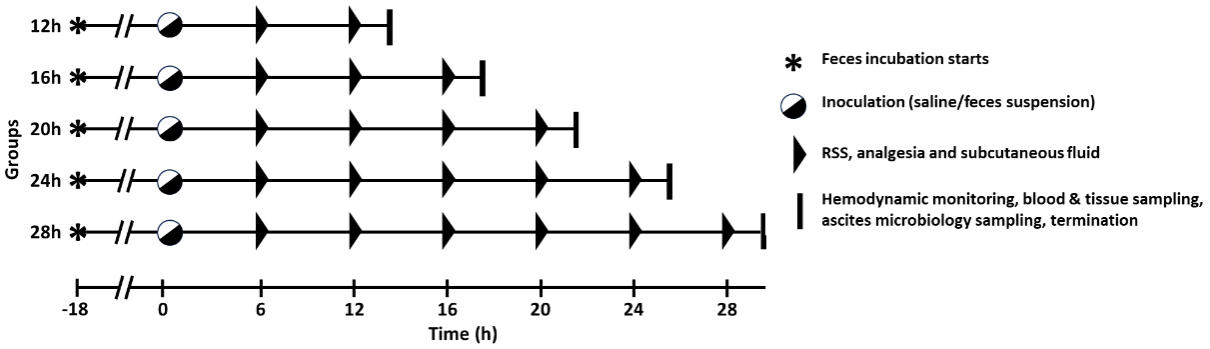

Figure 3. Experimental protocol and groups in Study 2. The animals were randomly assigned to sham-operated ($n_{\Sigma} = 40$) and septic groups ($n_{\Sigma} = 40$), which were randomly further divided into five independent subgroups each ($n_{12h} = 8$, $n_{16h} = 8$, $n_{20h} = 8$, $n_{24h} = 8$, and $n_{28h} = 8$) according to the different time points of sepsis progression. Following 6, 12, 16, 20, or 24h of sepsis progression, the animals were administered fluid therapy and analgesia (Ringerfundin, B. Braun, Hungary; Bupaq, Merck, USA; respectively) and RSS was evaluated. Subsequently, the animals were anesthetized, and invasive hemodynamic monitoring was initiated. Thereafter, a median laparotomy was performed to observe the ileal microcirculation with a serosal orientation (see Section 3.8). Immediately after microcirculatory measurements, a liver tissue biopsy was taken to assess mitochondrial respiratory functions (see Section 3.9). Afterward, blood samples were collected from the inferior vena cava to measure inflammatory and organ failure markers (see Section 3.7).

3.6. Anesthesia, surgical preparation, and invasive cardiopulmonary monitoring

In both studies, the animals were subjected to anesthesia by ip injection of a mixture of ketamine (45.7 mg kg^{-1}) and xylazine (9.1 mg kg^{-1}). Thereafter, the animals were positioned supine on a heating pad set to 37°C. Tracheostomy was performed, with the right jugular vein cannulated for fluid infusion (10 mL $kg^{-1}h^{-1}$ Ringerfundin) and continuous anesthesia (12.2 mg $kg^{-1}h^{-1}$ ketamine, 2.5 mg $kg^{-1}h^{-1}$ xylazine, and 0.61 mg $kg^{-1}h^{-1}$ diazepam iv). The left carotid artery was cannulated to monitor MAP, and a thermistor-tip catheter was inserted into the contralateral carotid artery to measure CO (Cardiosys 1.4, Experimetria Ltd., Budapest, Hungary). CO was adjusted by body weight, and hemodynamic parameters were recorded for the duration of the 60-min observation period. At the 60th min of the monitoring period, arterial blood samples were collected for blood gas analysis (Cobas b123; Roche Ltd., Basel, Switzerland). DO_2, VO_2, and ExO_2 were calculated using standard equations (Equation 1). Lung function was assessed by determining the ratio of arterial partial pressure of oxygen to the fraction of inspired oxygen (PaO_2 FiO_2^{-1}, where FiO_2 = 0.21). Following the 60-min hemodynamic monitoring, a median laparotomy was conducted to observe the microcirculation of the ileal serosa. Immediately after microcirculatory measurements, a liver tissue sample was taken to assess mitochondrial respiratory functions.

$$DO_2 = \mathrm{CO} \times [(1.38 \times \mathrm{Hb} \times SaO_2) + (0.003 \times PaO_2)$$

$$VO_2 = \mathrm{CO} \times [(1.38 \times \mathrm{Hb} \times (SaO_2 - SvO_2)) + (0.003 \times PaO_2)]$$

$$ExO_2 = DO_2\, {VO_2}^{-1}$$

Equation 1. Standard formulas used to calculate the parameters of global oxygen dynamics, where Hb is hemoglobin concentration, SaO_2 is oxygen saturation of the arterial blood, and SvO_2 is oxygen saturation of the venous blood.

3.7. Measurement of serum markers; assessment of ROFA score

Whole blood lactate levels were measured from venous blood (Accutrend Plus Kit; Roche Diagnostics Ltd., Rotkreuz, Switzerland). Blood samples were collected from the inferior vena cava in EDTA-coated tubes (1 mg mL^{-1}), centrifuged (1.200g at 4°C for 10 min), and stored at −70°C. Plasma IL-6 level and endothelin-1 (ET-1) levels were determined according to standard enzyme-linked immunosorbent assay kit protocols (Cusabio Biotechnology Ltd., Wuhan, China). Kidney function was characterized by plasma urea level. Liver function was assessed by plasma alanine aminotransferase (ALT) and aspartate aminotransferase (AST) levels (Roche/Hitachi 917 analyzer; F. Hoffmann–La Roche AG, Switzerland). A rat-specific organ failure assessment (ROFA) scoring system was used to describe the severity of MOF (Table 3) in accordance with the considerations of the MQTiPSS consensus guidelines. Sepsis was defined as a cumulative ROFA score over 2 (Rutai et al. 2020; Tallósy et al. 2021).

Table 3. Threshold values for the components of the rat-specific organ failure assessment (ROFA) scoring system. Sepsis was defined as a cumulative ROFA score above 2.

ROFA score	Plasma lactate (mmol L^{-1})	MAP (mmHg)	PaO_2 FiO_2^{-1} ratio	Plasma ALT (U L^{-1})	Plasma urea (mmol L^{-1})
0	< 1.64	> 75	> 400	< 17.5	< 7.5
1	1.64–3	65–75	300–400	17.5–30.2	7.5–21
2	3–4	55–65	200–300	> 30.2	> 21
3	4–5	< 55	100–200	–	
4	> 5	–	< 100	–	

3.8. Examination of ileal microcirculation with Incident Dark Field imaging

Ileal microcirculation was visualized with a serosal orientation using the Incident Dark Field (IDF) imaging technique (CytoCam Video Microscope System; Braedius Medical, Huizen, the Netherlands). After the median laparotomy (see Section 3.6), an ileal loop was removed from the abdomen intact and placed on a special holder, with an emphasis on avoiding stretching the organ and causing artificial circulatory damage in the mesenterium. The tissue was kept moist throughout the examination. The CytoCam device consists of LEDs emitting guided light with a wavelength of 530 nm, which is absorbed by hemoglobin-containing particles (red blood cells). Thanks to the real-time tracking, IDF differentiates the rate of blood

flow from the movement of the red blood cells. Images from an ileum segment were recorded in six, 50-frame, high-quality video clips. The records were analyzed with an offline software-assisted system. The proportion of perfused vessels (PPV) was defined as the ratio of the perfused vessel lengths to total vessel lengths (Aykut et al. 2015; De Backer et al. 2022). To evaluate microcirculatory heterogeneity, after a semiquantitative analysis, individual vessels were distinguished between (0) no flow, (1) intermittent flow, (2) sluggish flow, and (3) continuous flow. A value was assigned to each vessel and the overall score for each record was the average of the individual values, indicating the microvascular flow index (MFI). The heterogeneity index (HI) was defined as the difference between the highest MFI and the lowest MFI divided by the average MFI of the record (Ince et al. 2018; Pozo et al. 2012). The equations used to calculate the microvascular parameters are shown in Equation 2.

$$\boldsymbol{PPV} = \frac{Length\ of\ perfused\ vessels}{Length\ of\ all\ recorded\ vessels}\ x\ 100$$

$$\boldsymbol{HI} = \frac{highest\ MFI\ value - lowest\ MFI\ value}{average\ MFI\ value}$$

Equation 2. Equations used to calculate the microvascular variables

3.9. Assessment of hepatic mitochondrial functions with high-resolution respirometry

In both studies, mitochondrial oxygen consumption ($mtVO_2$) was measured in liver homogenates using high-resolution fluorespirometry (Oxygraph-2k, Oroboros Instruments, Innsbruck, Austria). In brief, liver samples obtained from the left lateral lobe were homogenized, and then respirometry was performed in a MiR05 respiration medium at a constant temperature with continuous stirring (37°C, 750 rpm) (Figure 4). After stabilization of VO_2, rotenone was added (1) to inhibit Complex I activity and (2) to prevent accumulation of oxaloacetate (a known endogenous inhibitor of Complex II). $FADH_2$-supported LEAK respiration and maximal capacity of oxidative phosphorylation (OxPhos) were determined in the presence of exogenous succinate and adenosine diphosphate (ADP). Following stimulation of OxPhos, the integrity of the mitochondrial outer membrane (mtOM) was tested with the addition of exogenous cytochrome c, and the increase in $mtVO_2$ was expressed as a percentage of $mtVO_2$ as compared to $mtVO_2$ in OxPhos (CytC%). Complex V (or ATP synthase) was inhibited by oligomycin to assess leak respiration in a non-phosphorylating state ($LEAK_{Omy}$) and to calculate respiratory control ratio (RCR), an index of the coupling of mitochondrial respiration to OxPhos ($Oxphos/LEAK_{Omy}$). DatLab 7.3.0.3. software (Oroboros Instruments, Innsbruck, Austria) was used for online display and respirometry data acquisition and analysis.

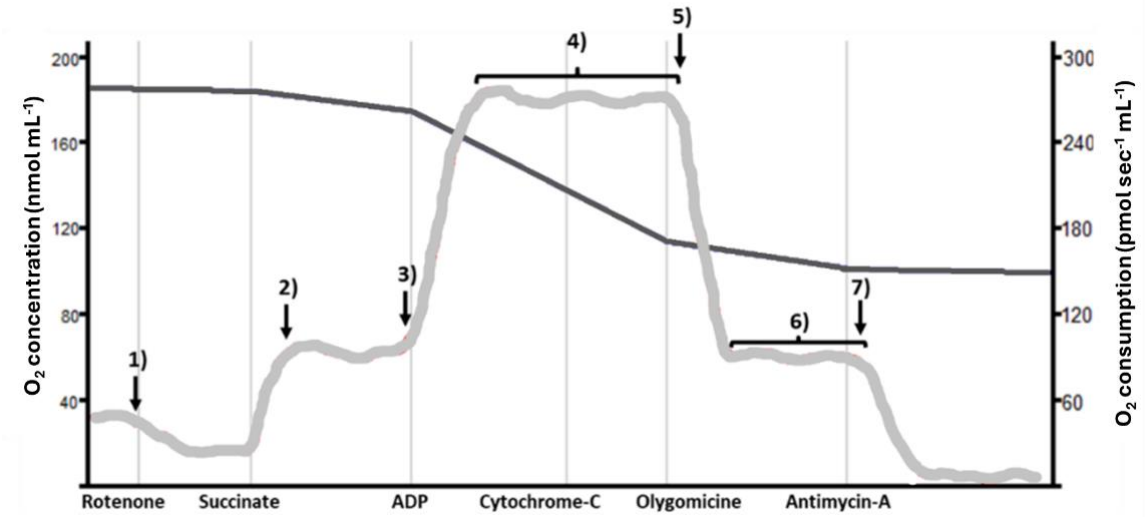

Figure 4. Protocol of a Complex II-specific Oxygraph-2k measurement. The dark gray, straight line indicates the O_2 concentration measured in the chamber, while the light gray, curved line indicates the O_2 consumption derived from the previous one. **1)** Inhibition of complex I by rotenone; **2)** Stimulation of Complex II-linked respiration by succinate; **3)** Addition of ADP to stimulate OxPhos; **4)** State 3, or maximal oxidative capacity; **5)** Inhibition of OxPhos by oligomycin; **6)** State 4, or leak respiration, indicating a non-phosphorylating respiration; **7)** Uncoupling the entire electron-transport chain: residual oxygen consumption, indicating non-mitochondrial (e.g., bacteria or inorganic oxidation) VO_2.

3.10. Statistical analysis

Data were evaluated with the SigmaStat 13 software package (Systat Software, San Jose, CA). The survival rate was analyzed and plotted using the Kaplan–Meier method. The Mann–Whitney or Kruskal–Wallis test was used with Dunn's post-hoc test for discrete variables, while a two-way ANOVA was employed for continuous variables followed by the Holm–Sidak post-hoc test. Data were displayed as median values and interquartile ranges between the 75th and 25th percentiles, with $P < 0.05$ being considered significant. The receiver operating characteristic (ROC) curve analysis was used to represent the diagnostic accuracy of the different parameters determined by the area under the curve (AUC) data (GraphPad Prism 8.0). A multivariate analysis model was performed with a logical data analysis method and data processing with GraphPad Prism 8.0 software. Pearson's method or Spearman's methods were employed to analyze the linear correlation, correlation coefficient (r), regression lines, and 95% confidence intervals.

4. Results

4.1. Study 1

4.1.1. Animal well-being; mortality

The RSS score did not change significantly at 12h after the septic challenge (Figure 5a), and there was no mortality in these groups (Figure 5b). Within 24h, the condition of some septic animals deteriorated significantly, RSS reached a critical value of 6 (i.e., the threshold for a humane endpoint), and therefore n = 3, n = 4, and n = 3 animals were euthanized in Groups 24h, 48h, and 72h, respectively. The numbers of euthanized animals are included in the mortality calculations (Figure 5b). The general condition of the surviving septic animals did not deteriorate between 48 and 72h.

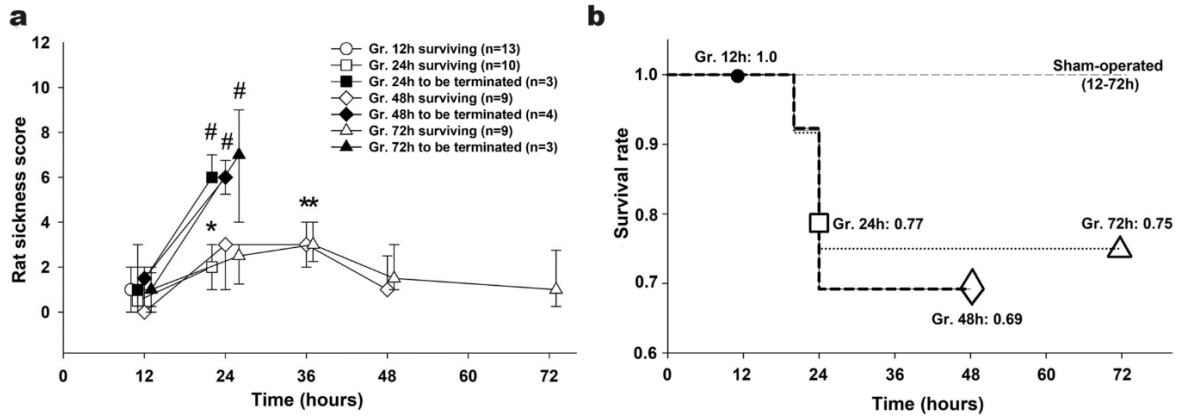

Figure 5. Rat-specific sickness score (RSS) and mortality at different stages of the sepsis. **(a)** Within the septic animals, the RSS score values for the surviving animals (open symbols) and those reaching the threshold value of 6 (euthanized subjects; black symbols) are shown separately. Plots demonstrate the median values and the 25th and 75th percentiles. Within groups: the Friedman test and Dunn's post-hoc test. $^{*}P < 0.05$ *vs.* non-lethal 12h sepsis. Between groups: Mann–Whitney U test. $^{\#}P < 0.05$ lethal *vs.* non-lethal sepsis at 24h. **(b)** The survival rates are indicated for the Kaplan–Meier survival analysis on the four sepsis groups (Groups 12h, 24h, 48h, and 72h) and four sham-operated groups.

4.1.2. Global and subcellular oxygen dynamics; inflammatory markers

There was no significant difference in ExO_2 between the sham-operated and septic animals at 12h, but the values showed a significant reduction after 24h of sepsis (Figure 6a). In the septic groups, less diminished ExO_2 values were detected. The Complex II-linked OxPhos also shows deterioration in the 24h septic animals only (Figure 6b*; $P < 0.01$*). Elevated levels of plasma IL-6 were observed 12h after induction (Figure 6c; $P = 0.018$); plasma ET-1 concentration increased significantly at 24h of sepsis (Figure 6d).

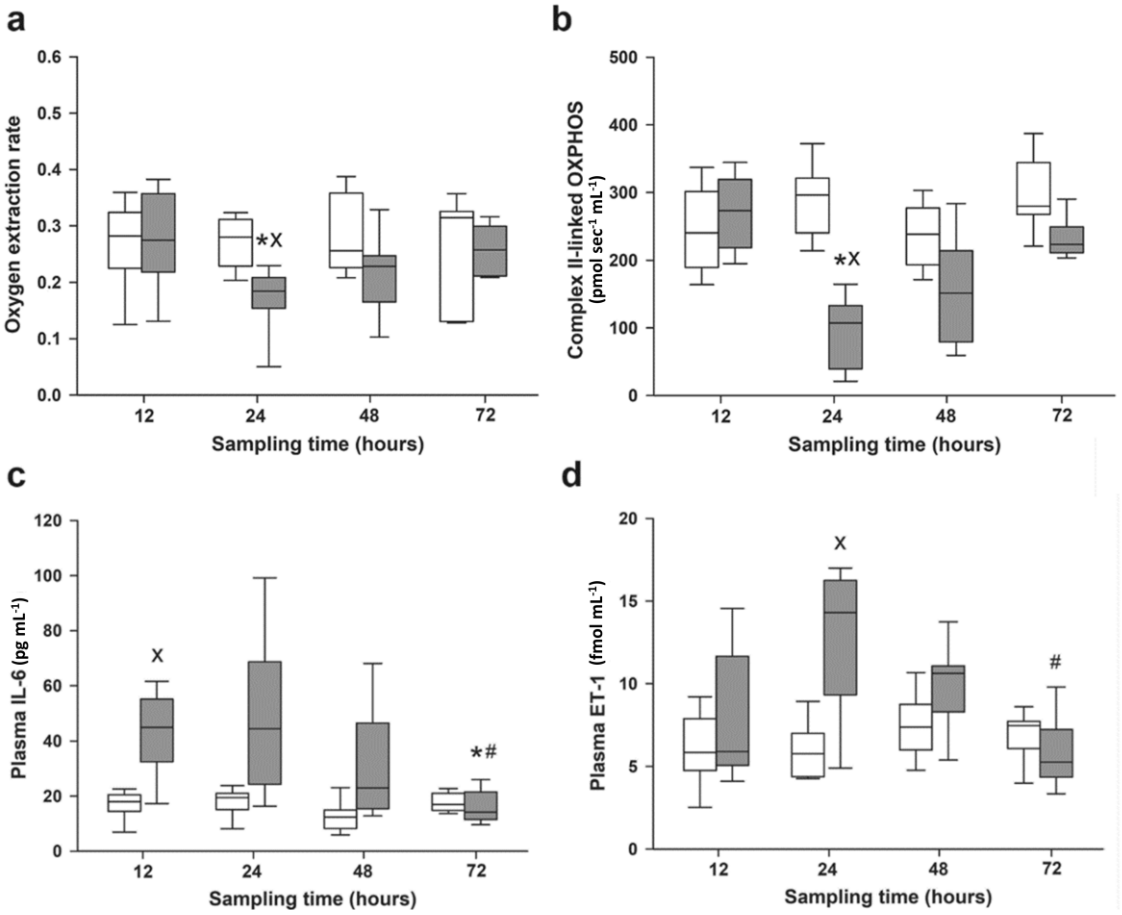

Figure 6. **(a)** Global oxygen extraction (ExO_2), **(b)** Complex II-linked oxidative phosphorylation (OxPhos), **(c)** plasma interleukin-6 (IL-6), and **(d)** endothelin-1 (ET-1) concentrations in the sham-operated animals (n = 12–13, white boxes) and in the different sepsis groups (gray boxes). Plots demonstrate the median and the 25th and 75th percentiles. A comparison between groups was conducted with the Kruskal–Wallis test followed by Dunn's post-hoc test. $^{X}P < 0.05$ *vs.* sham-operated; $*P < 0.05$ *vs.* 12h sepsis (between sepsis groups); $^{\#}P < 0.05$ *vs.* 24h sepsis (between sepsis groups).

4.1.3. Changes in ROFA score

The ROFA score showed significant increases at 24 and 48h (Figure 7). Deteriorations in the 24h values were attributable to all parameters examined, whereas similar changes were also present for most parameters at 48h, except for the non-significantly different whole blood lactate and plasma ALT values. ROFA scores returned to the values for the sham-operated animals after 72h.

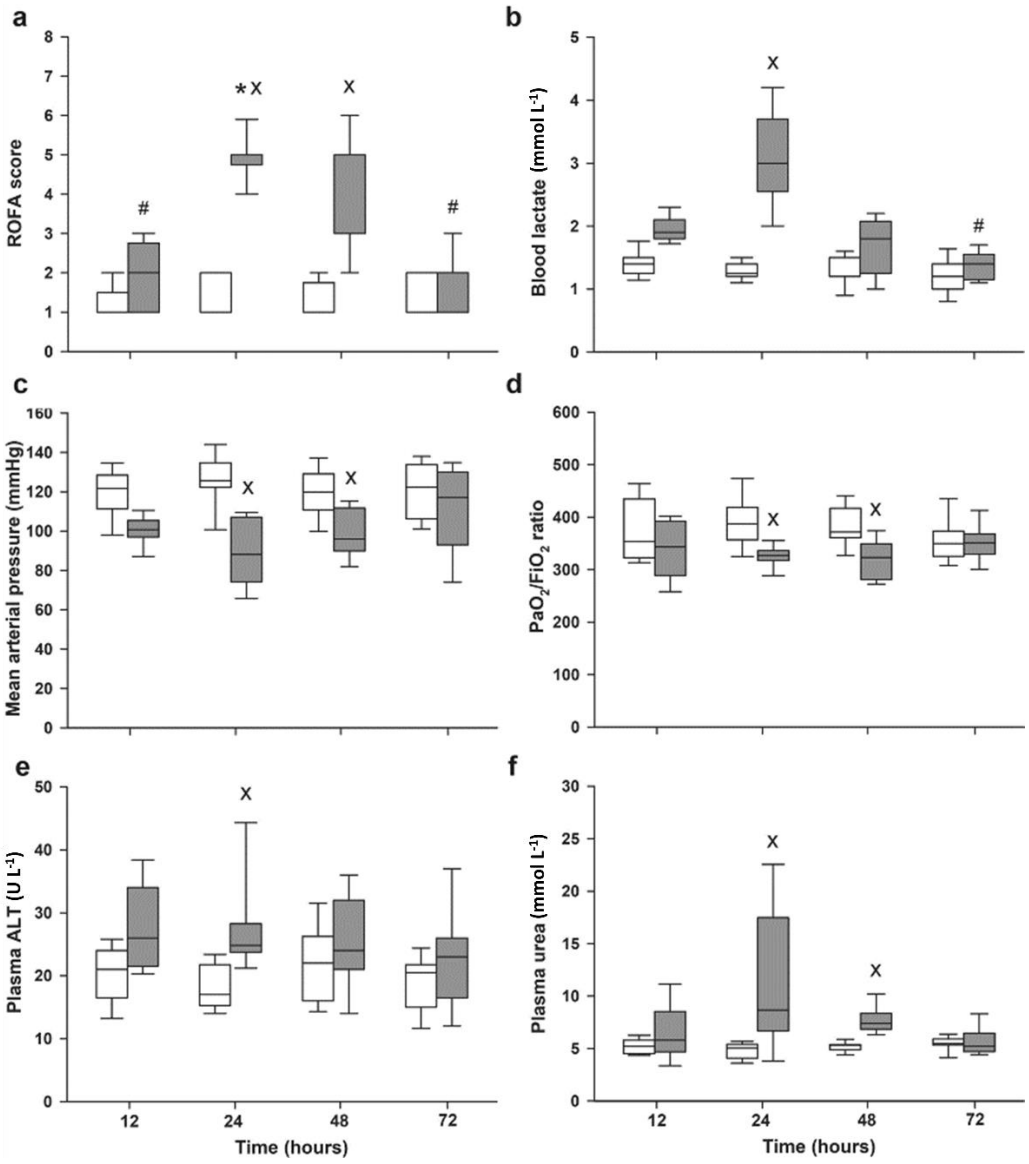

Figure 7. Rat-specific organ failure assessment (ROFA) score and its components in the sham-operated animals (white boxes) and in the different sepsis groups (gray boxes). Cumulative **(a)** ROFA score, **(b)** whole blood lactate level, **(c)** mean arterial pressure, **(d)** lung injury, **(e)** plasma alanine aminotransferase (ALT), and **(f)** plasma urea levels are shown. Comparisons between groups were conducted with the Kruskal–Wallis test followed by Dunn's post-hoc test. $^{X}P < 0.05$ *vs.* sham-operated; $^{*}P < 0.05$ *vs.* 12h sepsis (between sepsis groups); $^{\#}P < 0.05$ *vs.* 24h sepsis (between sepsis groups).

4.1.4. Microbial background of the fecal inoculum and the ascites

In addition to determining CFU, analysis of the bacterial pattern was performed from both the sepsis-inducing fecal inocula and the ascites (the latter taken upon termination in Groups 12–72h). This retrospective microbial analysis revealed that, despite the statistically similar bacterial doses, marked qualitative differences in bacterial composition and monomicrobial/polymicrobial pattern existed in the composition of the inocula (Figure 8 and Table 4). It was proven that only E. coli was present in 20% of inocula ($n_{\Sigma} = 10$) and all early (24h) sepsis mortality was attributable to injection with E. coli monomicrobial cultures. In the sepsis-inducing inocula, three bacterial phyla, including 18 mostly Gram-negative genera, could be detected. Specifically, most taxa belonged to Proteobacteria (49%; e.g., E. coli), and the rest were distributed among the Firmicutes (38%; e.g., Lactobacilli) and Actinobacteria (13%; e.g., *Propionibacterium acnes*). The most frequent strains in the inducer inoculum were *E. coli* (in 100% of the samples), followed by *Klebsiella pneumoniae*, Pseudomonas, Bifidobacteria, and Lactobacilli. In the ascites, bacterium concentration decreased by one order of magnitude ($P < 0.01$), which was accompanied by reduced diversity of bacterial strains. New species also reached the detection level. After 72h of sepsis, only E. coli (in 100% of the samples) and *Lactobacillus murinus* (in 17% of the samples) were identified in the ascites.

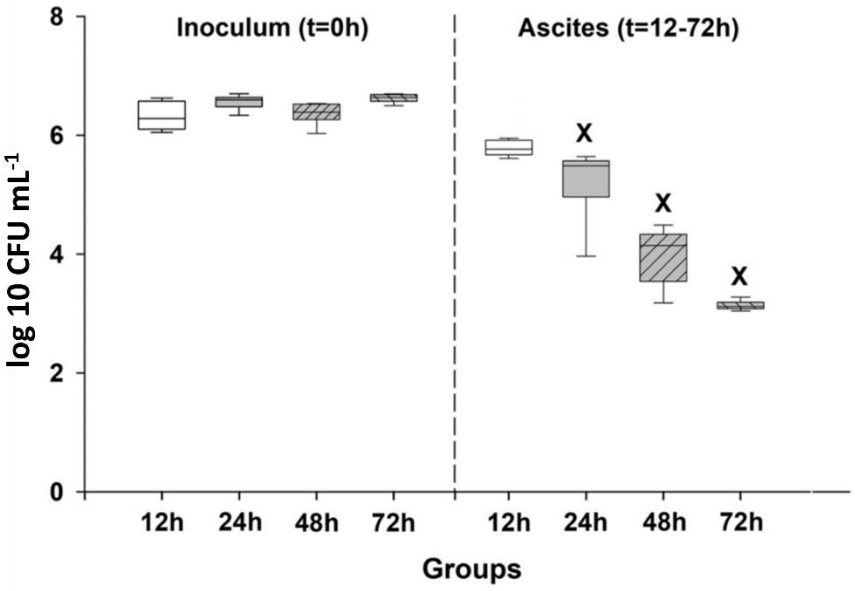

Figure 8. Bacterium concentration in the induction inocula and the ascites in the different sepsis groups. Plots demonstrate the median and the 25th and 75th percentiles. Data were analyzed with two-way analysis of variance followed by the Holm–Sidak post-hoc test. $^{X}P < 0.05$ *vs.* corresponding inducer inoculum.

Table 4. Bacterium composition in the fecal inoculum and the ascites. Bacterial composition of fecal inoculum (Inoc.) and ascites (Asc.) expressed as an incidence of the actual strain per total number of samples (%) in the different sepsis groups.

Species	Groups							
	Group 12h		Group 24h		Group 48h		Group 72h	
	Inoc. (n=13)	Asc. (n=13)	Inoc. (n=13)	Asc. (n=10)	Inoc. (n=13)	Asc. (n=9)	Inoc. (n=12)	Asc. (n=9)
Gram-negative species								
Acinetobacter radioresistens	92	50	71	33	68	0	67	0
Acinetobacter sp.	33	0	42	0	8	0	33	0
Aeromonas caviae	33	0	42	0	8	0	25	0
Brevundimonas diminuta	33	0	33	0	17	0	17	0
Escherichia coli	100	100	100	100	100	100	100	100
Klebsiella pneumoniae	92	0	75	0	65	0	72	0
Neisseria subflava	0	67	0	29	0	33	0	0
Pseudomonas aeruginosa	90	31	73	21	33	0	25	0
Pseudomonas mucidolens	33	0	42	0	8	0	0	0
Pseudomonas stutzeri	33	0	25	0	33	0	67	0
Ralstonia pickettii	0	32	0	33	0	0	0	0
Stenotrophomonas maltophilia	67	30	75	33	0	0	8	0
Veilonella criceti	0	0	0	0	33	0	25	0
Gram-positive species								
Bifidobacterium animalis	33	79	25	61	33	33	67	0
Enterococcus ratti	17	0	4	0	8	0	54	0
Enterococcus faecium	8	67	8	33	42	0	33	0
Enterococcus gallinarum	0	0	0	0	33	0	33	0
Lactobacillus intestinalis	90	0	68	0	67	0	67	0
Lactobacillus murinus	33	83	33	62	50	60	68	17
Lactobacillus johnsonii	8	0	0	0	67	0	33	0
Lactobacillus mali	8	0	0	0	33	0	33	0
Lactobacillus garvieae	0	0	0	0	0	0	33	0
Micrococcus luteus	33	83	0	67	33	48	17	0
Proprionibacterium acnes	8	0	4	0	17	0	0	0
Staphylococcus aureus	50	30	75	8	25	42	17	0
Staphylococcus hominis	67	0	58	0	8	0	0	0
Streptococcus hyointestinalis	67	0	58	0	0	0	0	0

4.1.5. Association between the inducing bacterial dose and the severity of organ failure

The initial CFU and ROFA scores showed a moderate relationship at 12h (Figure 9a). However, a significant correlation between these parameters was observed at 24h of fecal peritonitis (Figure 9b). No connection between the amount of injected CFU and ROFA score was found at 48 and 72h (Figure 9c and d).

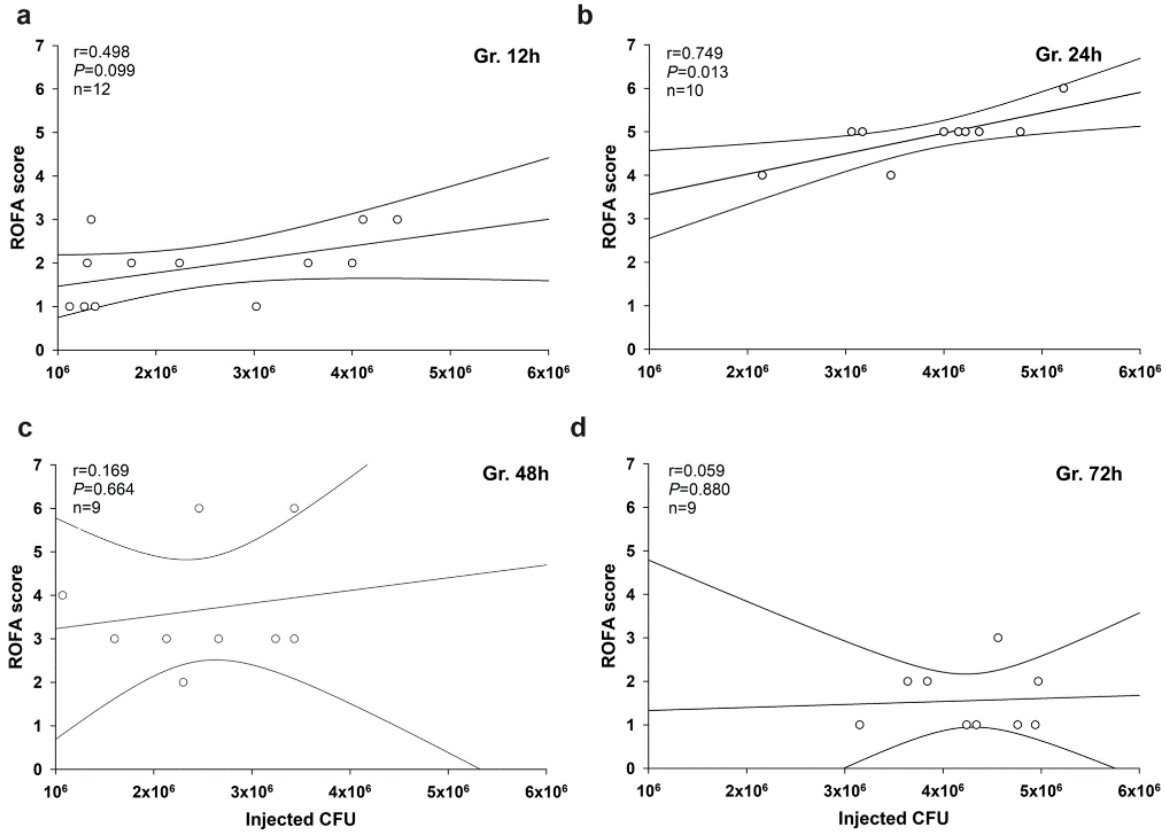

Figure 9. Correlation between the CFU values for the inducer inoculum and ROFA scores. Values are shown in the **(a)** 12h, **(b)** 24h, **(c)** 48h, and **(d)** 72h polymicrobial sepsis groups. Pearson's correlation coefficient r values and (null hypothesis-related) *P* values are provided, and regression lines and 95% confidence intervals are indicated.

4.1.6. ROFA score components at 24h after mono- and polymicrobial inocula

Since marked differences in the diversity of bacterial strains were revealed in the inoculum, we ran a retrospective subgroup analysis to compare the parameters of the ROFA scores for animals that were found to be challenged with polymicrobial inoculum (in the 24h sepsis group; n = 10) and with E. coli monomicrobial content in the 24, 48, and 72h sepsis groups (n = 3, 4, and 3 animals, respectively). We found significantly higher ALT and ROFA score values in the animals injected with E. coli monomicrobial inoculum compared to the other cohort (Figure 10a–c). Bearing in mind the negligible quantitative differences in inocula but the differences in their microbiological diversity, we also retrospectively assessed how simultaneous consideration of these features influenced organ dysfunction at 24h of sepsis.

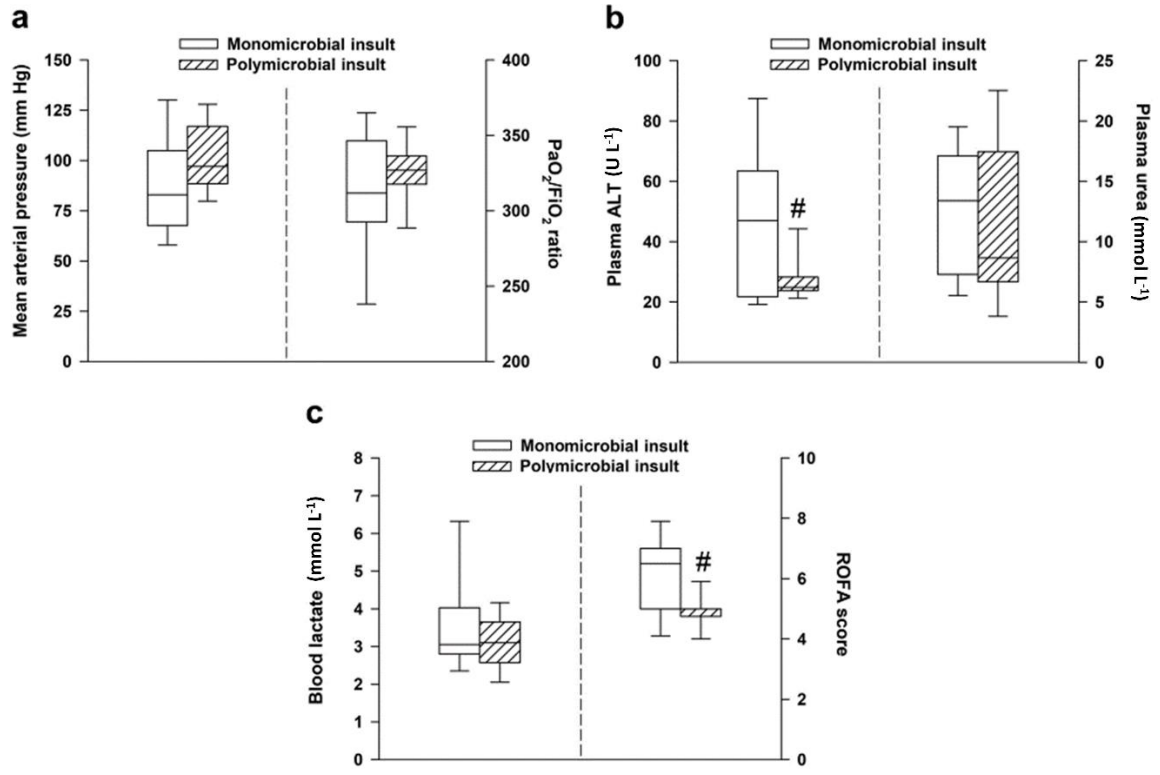

Figure 10. Comparison of **(a)** mean arterial pressure and lung injury, **(b)** plasma alanine aminotransferase (ALT) and plasma urea levels, and **(c)** blood lactate levels and cumulative ROFA score in the E. coli monomicrobial or polymicrobial subgroups at 24h. Plots demonstrate the median and the 25th and 75th percentiles. Between groups, a comparison of ROFA score values was made with the Mann–Whitney U test, whereas ROFA components were compared with the Welch independent samples t-test. $^{\#}P < 0.05$ monomicrobial *vs.* polymicrobial subgroups.

The relationship between the CFU values and ROFA scores showed a similar correlation in both the E. coli monomicrobial and the polymicrobial subgroups, but the slope of the regression line of the monomicrobial subgroup was greater than that of the polymicrobial subgroup (Figure 11a). Furthermore, the ROFA score also displayed a correlation with the ascites CFU values. A significant non-linear relationship was identified between the ascites CFU and the ROFA score in the polymicrobial or monomicrobial subgroups during the 12–72h sepsis period with a shifting of the bacterial composition towards E. coli dominance over time (Figure 11b).

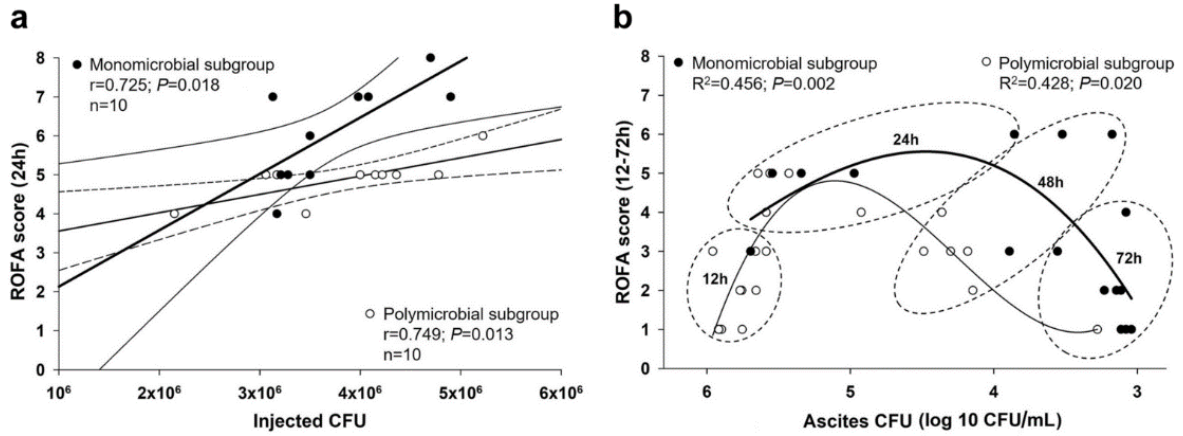

Figure 11. Correlations between inoculum and ascites CFU and ROFA score values in mono- or polymicrobial subgroups. **(a)** Correlations between CFU values for the mono- or polymicrobial inducer inoculum and ROFA scores at 24h of sepsis. The E. coli monomicrobial subgroup (n = 10) is marked with black circles, a thick regression line, and a thin line for the 95% confidence interval, whereas the polymicrobial subgroup (n = 10) is indicated with open circles, a thin regression line, and a dashed line for the 95% confidence interval. Pearson's product correlation coefficient r values, (null hypothesis-related) P values, and numbers of animals involved in the subgroup analysis are provided. **(b)** Relationship between the log 10 CFU values for ascites and ROFA score values in all septic groups. Evolving predominance of ascites monomicrobial (black circles) *vs.* polymicrobial (open circles) content and reduced CFUs in ascites over time. Polynomial regression curves of the polymicrobial and monomicrobial ascites samples are marked with a thin and a thick line, respectively. Third-order polynomial curve fit values (R^2 and *P*) are indicated. Data for different stages of sepsis are illustrated with dashed ellipses.

4.2. Study 2

4.2.1. Animal well-being and mortality

There were no significant changes in the RSS score in the sham-operated group. Septic groups between 20 and 24h elevated significantly not only compared to the 12h septic group but also compared to the 20 and 24h sham-operated groups (Figure 12a). Three animals were euthanized due to a critically elevated RSS score (Figure 12b).

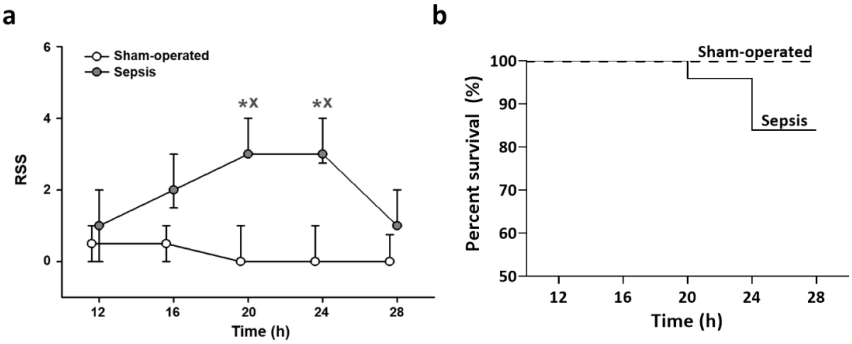

Figure 12. Rat-specific **(a)** well-being–related sickness score (RSS) and **(b)** mortality. **(a)** A comparison within groups was conducted with the Kruskal–Wallis test followed by Dunn's post-hoc test compared to the 12h group. The Mann–Whitney U test was performed between the sham-operated and septic groups at the same time point. **P* < 0.05 *vs.* sham-operated within the same time point, $^{X}P < 0.05$ *vs.* the 12h group within treatment. **(b)** Kaplan–Meier analysis was performed to describe the survival of the animals.

4.2.2. Changes in inflammatory and multi-organ failure markers

IL-6 significantly increased as compared to the sham-operated group, peaking at 16h ($P < 0.001$; Figure 13a), after which a decrease started reaching the level of the sham-operated group after 24h (Table 4). ROFA parameters were significantly higher in the septic groups compared to the sham-operated animals during the whole experimental period, with the score reaching the maximum at 20h ($P = 0.007$; Figure 13b).

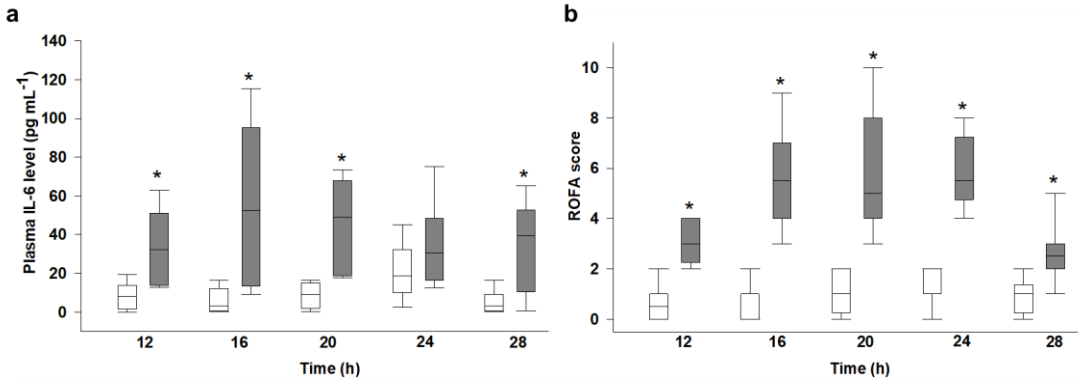

Figure 13. (a) Plasma interleukin-6 (IL-6) level and **(b)** the rat-specific organ failure assessment (ROFA) score in the sham-operated animal subgroups (white boxes) and the sepsis subgroups (gray boxes). The plots demonstrate the median and the 25th and 75th percentiles. Data were analyzed by two-way analysis of variance (ANOVA) followed by the Holm–Sidak post-hoc test. **P* < 0.05 *vs*. sham-operated at the same time point.

4.2.3. Changes in macrohemodynamics

In the sham-operated group, there were no significant hemodynamic changes over time. Sepsis was characterized by significant hypotension between 16 and 24h ($P_{16h} = 0.05$; $P_{20h} < 0.001$; $P_{24h} = 0.001$; Figure 14a) compared to the sham-operated animals at the same time points (Table 4). An increasing trend was observed in CO data until 16h ($P < 0.001$), and then CO dropped significantly below the level of the sham-operated animals at 20h ($P < 0.001$). Later, CO values did not differ from the sham-operated group. In the 16–24h interval, the CO values differed significantly from the values for the 12h group, albeit in a different way ($P_{16h} = 0.009$; $P_{20h} < 0.001$; $P_{24h} = 0.008$; Figure 14b).

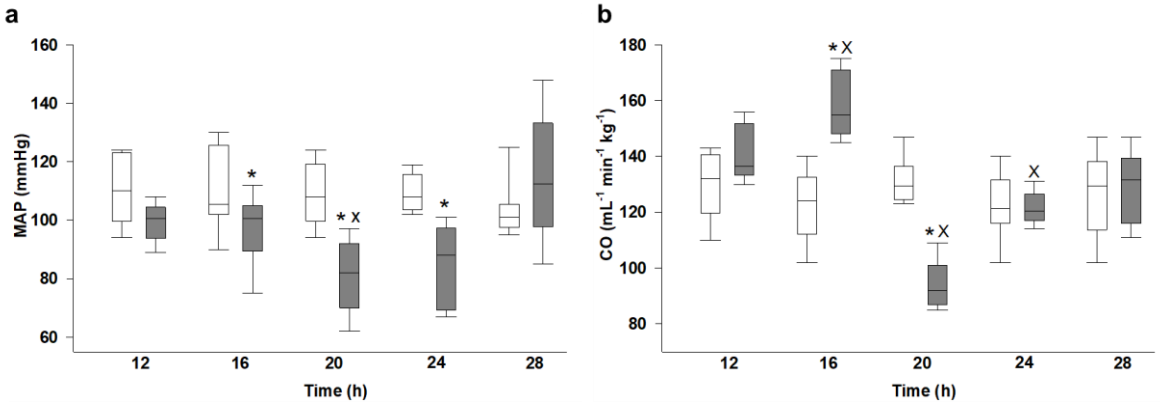

Figure 14. (a) Mean arterial pressure (MAP) and **(b)** cardiac output (CO) in the sham-operated animal subgroups (white boxes) and the sepsis subgroups (gray boxes). The plots demonstrate the median and the 25th and 75th percentiles. Data were analyzed by two-way analysis of variance (ANOVA) followed by the Holm–Sidak post-hoc test. *$P < 0.05$ *vs*. sham-operated at the same time point, $^{X}P < 0.05$ *vs*. the 12h sham-operated group.

4.2.4. Changes in oxygen dynamics

DO_2 showed a progressive decline in the septic group, reaching its lowest value at 20h, thereafter exceeding the levels for the sham-operated animals at 28h (Figure 15a). There was no significant change in VO_2 except at 16h ($P = 0.008$; Figure 15b). ExO_2 rose until 20h when the trend reversed and did not alter from the values for the sham-operated groups. In the 16–24h interval, the ExO_2 values differed significantly from the values for the 12h septic group ($P_{16h} = 0.035$; $P_{20h} < 0.005$; $P_{24h} = 0.039$; Figure 15c).

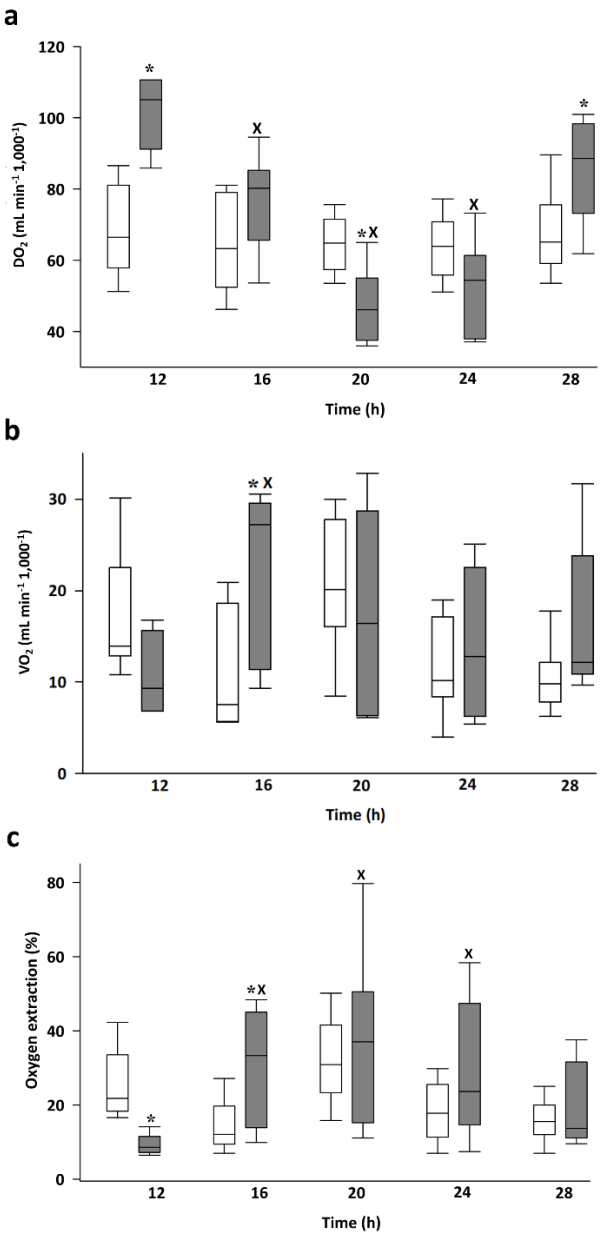

Figure 15. (a) Oxygen delivery (DO_2), **(b)** oxygen consumption (VO_2), and **(c)** oxygen extraction (ExO_2) in the sham-operated animal subgroups (white boxes) and the sepsis subgroups (gray boxes). The plots demonstrate the median and the 25th and 75th percentiles. Data were analyzed by two-way analysis of variance (ANOVA) followed by the Holm–Sidak post-hoc test. *$P < 0.05$ *vs*. sham-operated at the same time point, $^{X}P < 0.05$ *vs*. the 12h sham-operated group.

4.2.5. Changes in microhemodynamics

PPV ($P_{16h–28h}$ < 0.001; Figure 16a) and MFI were significantly higher ($P_{16h–28h}$ < 0.001; Figure 16b) as compared with those in the sham-operated group between the 16 and 28h intervals. HI was significantly higher in the 16–28h time window with a decreasing trend in the septic group but still significantly higher compared to the sham-operated group at 28h (P_{28h} = 0.003; Figure 16c).

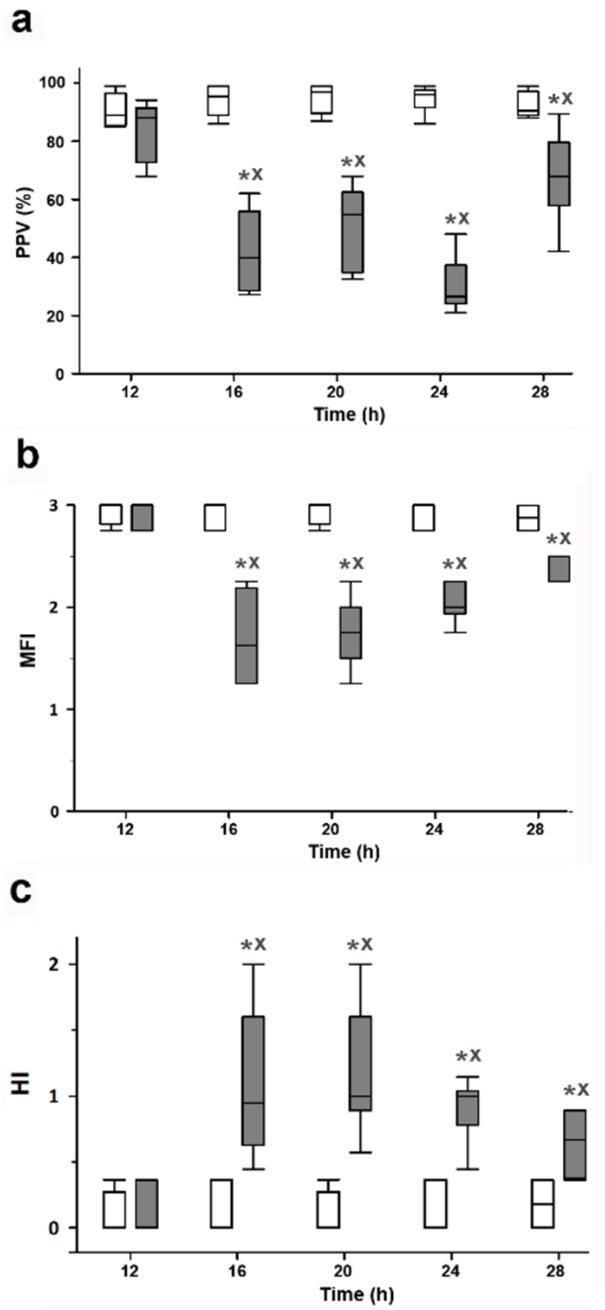

Figure 16. (a) The proportion of perfused vessels (PPV), **(b)** the microvascular flow index (MFI), and **(c)** the heterogeneity index (HI) in the sham-operated animal subgroups (white boxes) and the sepsis subgroups (gray boxes). The plots demonstrate the median and the 25th and 75th percentiles. Data were analyzed by two-way analysis of variance (ANOVA) followed by the Holm–Sidak post-hoc test. *P < 0.05 *vs*. sham-operated at the same time point, ^{X}P < 0.05 *vs*. the 12h sham-operated group.

4.2.6. Changes in liver mitochondrial functions

The OxPhos and $LEAK_{Omy}$ values for the septic animals significantly decreased at 20h (OxPhos: $P < 0.001$; $LEAK_{Omy}$: $P = 0.006$) compared to the sham-operated group (Figure 17a and b). CytC%, which characterizes mtOM damage, showed a strong increasing trend with a maximum at 20h ($P = 0.028$) and was significantly different from the sham-operated groups between 16 and 28h ($P_{16h–28h} < 0.001$; Figure 17c). RCR did not differ significantly in the septic animals compared to the sham-operated ones during the whole experimental period (Figure 17d).

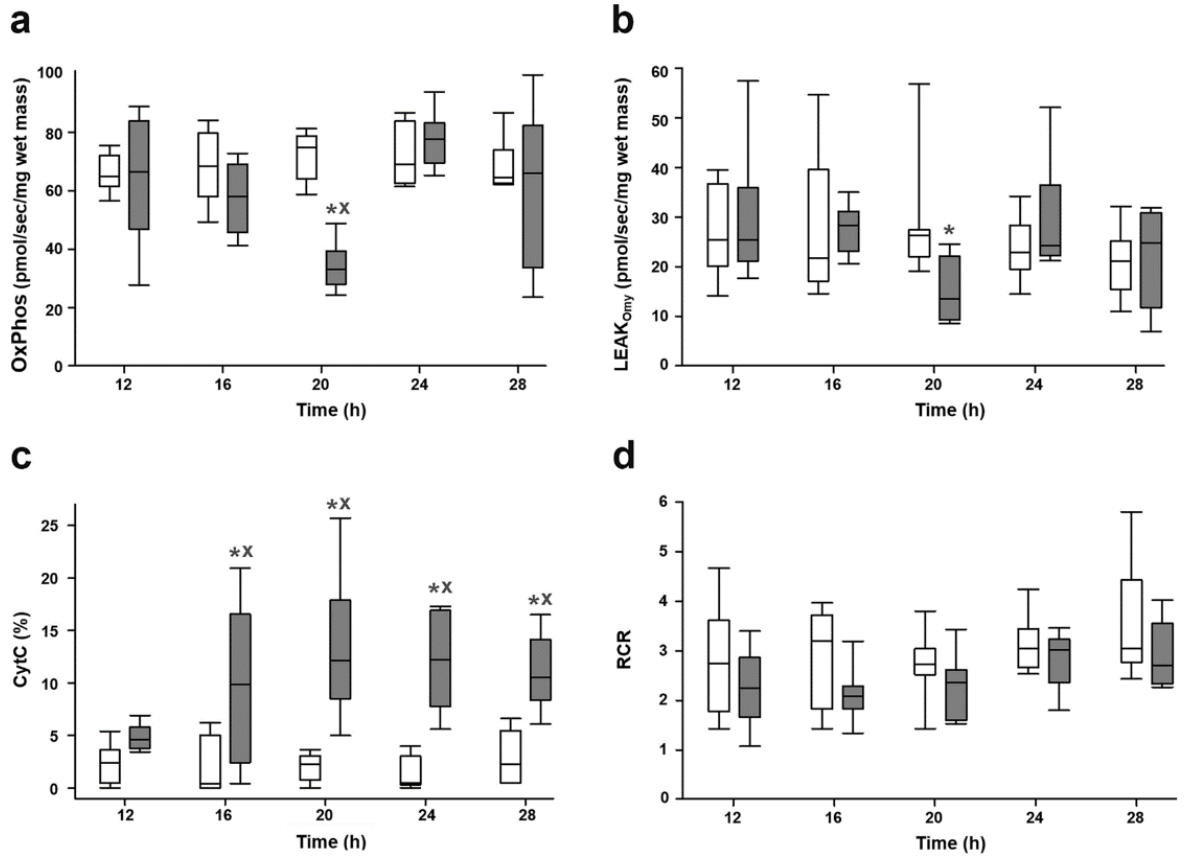

Figure 17. (a) Oxidative phosphorylation (OxPhos), **(b)** oligomycin-induced leak state ($LEAK_{Omy}$), **(c)** cytochrome c control efficiency (CytC%), and **(d)** the respiratory control ratio (RCR) in the sham-operated animal subgroups (white boxes) and the sepsis subgroups (gray boxes). The plots demonstrate the median (horizontal line in the box) and the 25th (lower whisker) and 75th (upper whisker) percentiles. Data were analyzed by two-way analysis of variance followed by the Holm–Sidak post-hoc test. *$P <$ 0.05 *vs*. sham-operated at the same time point, $^{X}P < 0.05$ *vs*. the 12h sham-operated group.

4.2.7. Receiver operating characteristic (ROC) curve analyses

The diagnostic power of the parameters was determined with the calculated AUC values from the ROC analysis. Among the parameters of the ROFA score (Figure 18a–e), only whole blood lactate level showed relevant predictive value ($AUC_{lactate}$ = 0.9054). Among the mitochondrial functions (Figure 18f–i), CytC% proved to be a strong predictor ($AUC_{CytC\%}$ = 0.9453). Among the microcirculatory parameters (Figure 18j–l), PPV showed the strongest predictive value (AUC_{PPV} = 0.9483); however, both MFI and HI had a particularly high predictive value (AUC_{MFI} = 0.8946; AUC_{HI} = 0.8851).

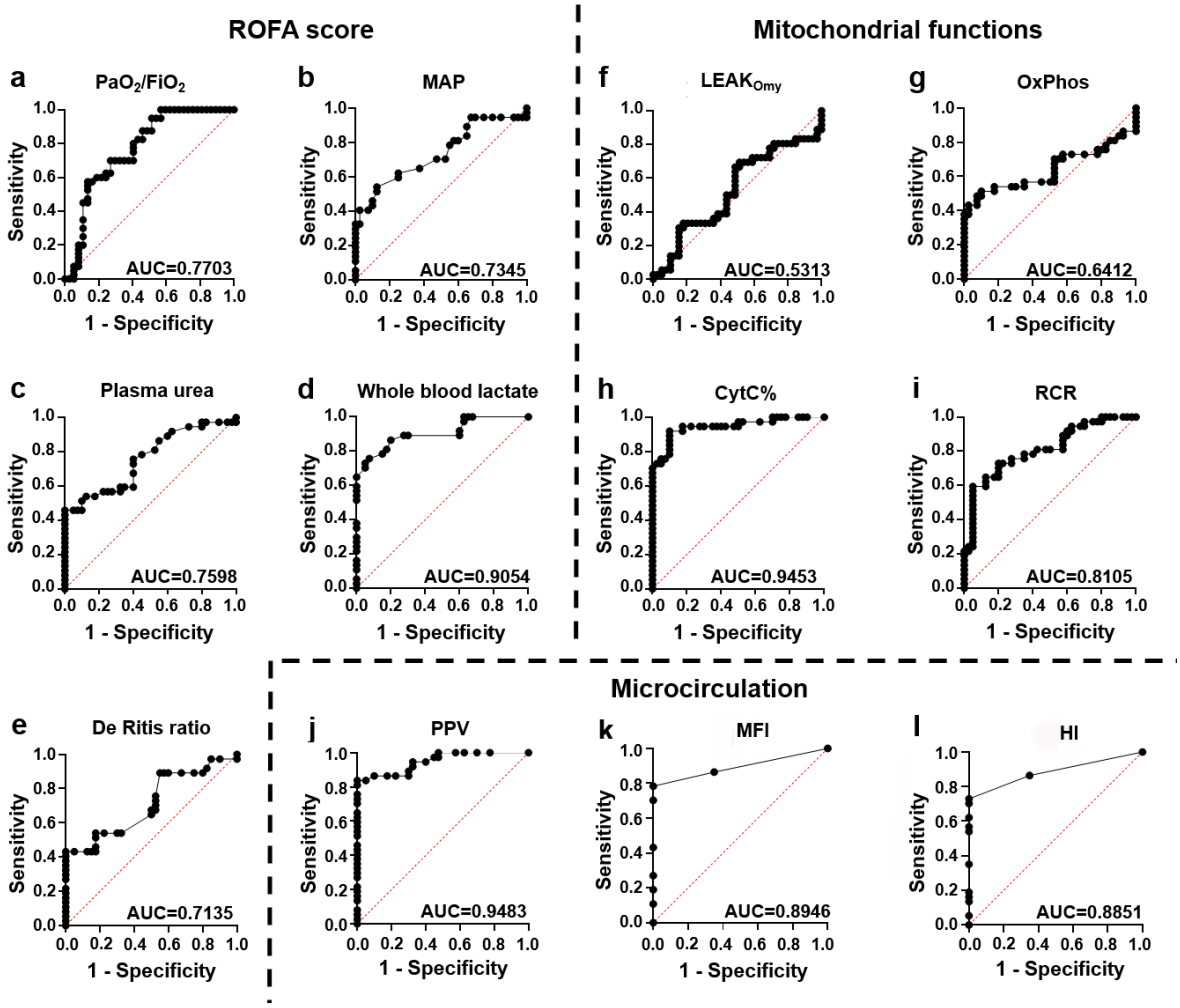

Figure 18. (a) ROC curve of the $PaO_2\,FiO_2^{-1}$ ratio, **(b)** mean arterial pressure (MAP), **(c)** plasma urea level, **(d)** whole blood lactate level, **(e)** DeRitis ratio, **(f)** oligomycin-induced leak respiration ($LEAK_{Omy}$), **(g)** oxidative phosphorylation (OxPhos), **(h)** cytochrome c control efficiency (CytC%), **(i)** the respiratory control ratio (RCR), **(j)** the proportion of perfused vessels (PPV), **(k)** the microvascular flow index (MFI), and **(l)** the heterogeneity index (HI).

4.2.8. Correlation between mitochondrial and microcirculatory parameters and the ROFA score

There was no significant correlation in the sham-operated groups. There was a negative, significant correlation between PPV and the ROFA score (r = -0.484, *P* = 0.00259; Figure 19a) and a positive, significant correlation between HI and the ROFA score (r = 0.520, *P* = 0.00106; Figure 19b). There were no relations between the mitochondrial parameters and the ROFA score (Figure 19c and d).

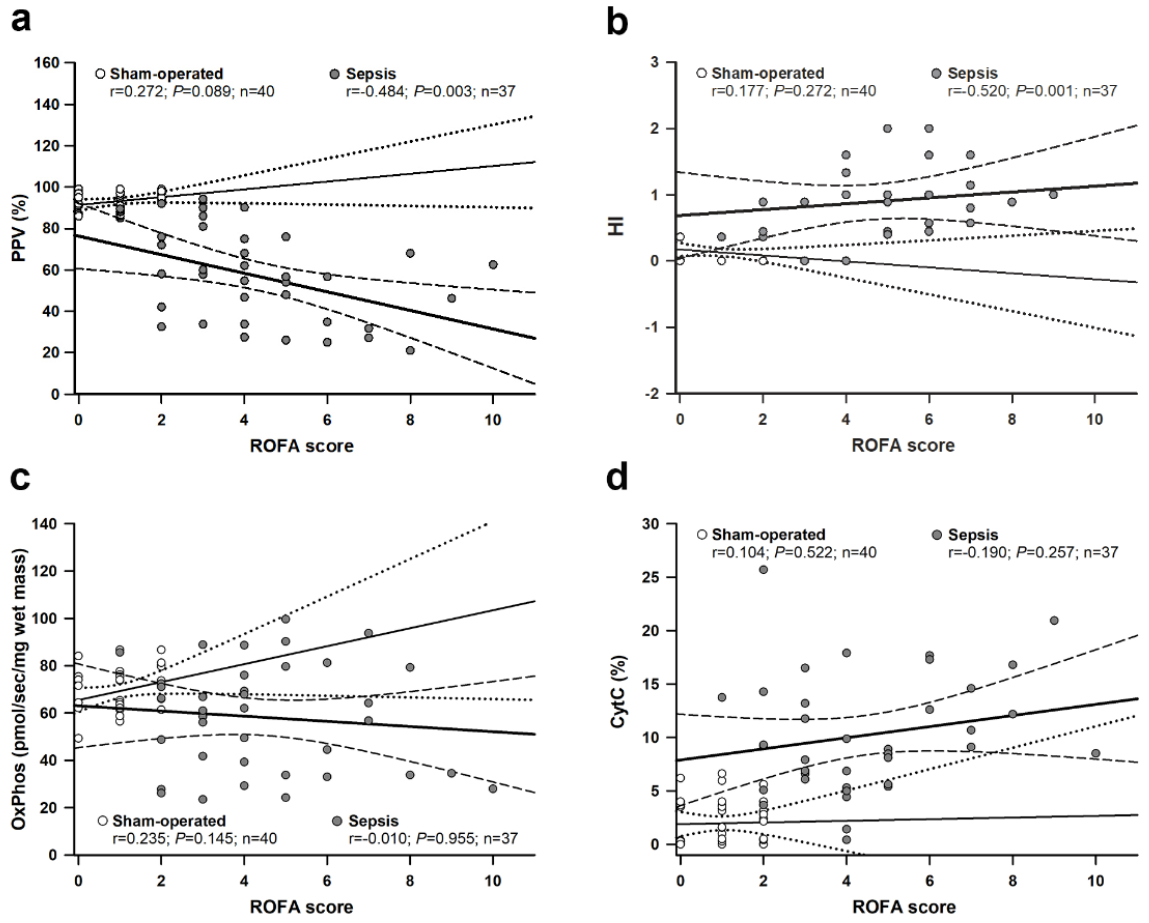

Figure 19. Correlation between the ROFA score and microcirculatory parameters (**a:** proportion of perfused vessels [PPV]; **b:** heterogeneity index [HI]) or mitochondrial functions (**c:** oxidative phosphorylation [OxPhos]; **d:** cytochrome c control efficiency [CytC%]) were examined by the Spearman correlation test. Correlation coefficient r values, (null hypothesis-related) *P* values, and numbers of animals involved in the sham-operated and septic groups are provided with a 95% confidence interval.

4.2.9. Correlation between mitochondrial and microcirculatory parameters

There was no significant correlation in the sham-operated groups. There was no significant correlation between the microcirculation and OxPhos variables (Figure 20a and b). There was a negative, significant correlation between PPV and CytC% (r = -0.505, $P = 0.00153$; Figure 20c); however, HI and CytC% also showed a moderate positive relationship (r = 0.332, $P = 0.0445$; Figure 20d).

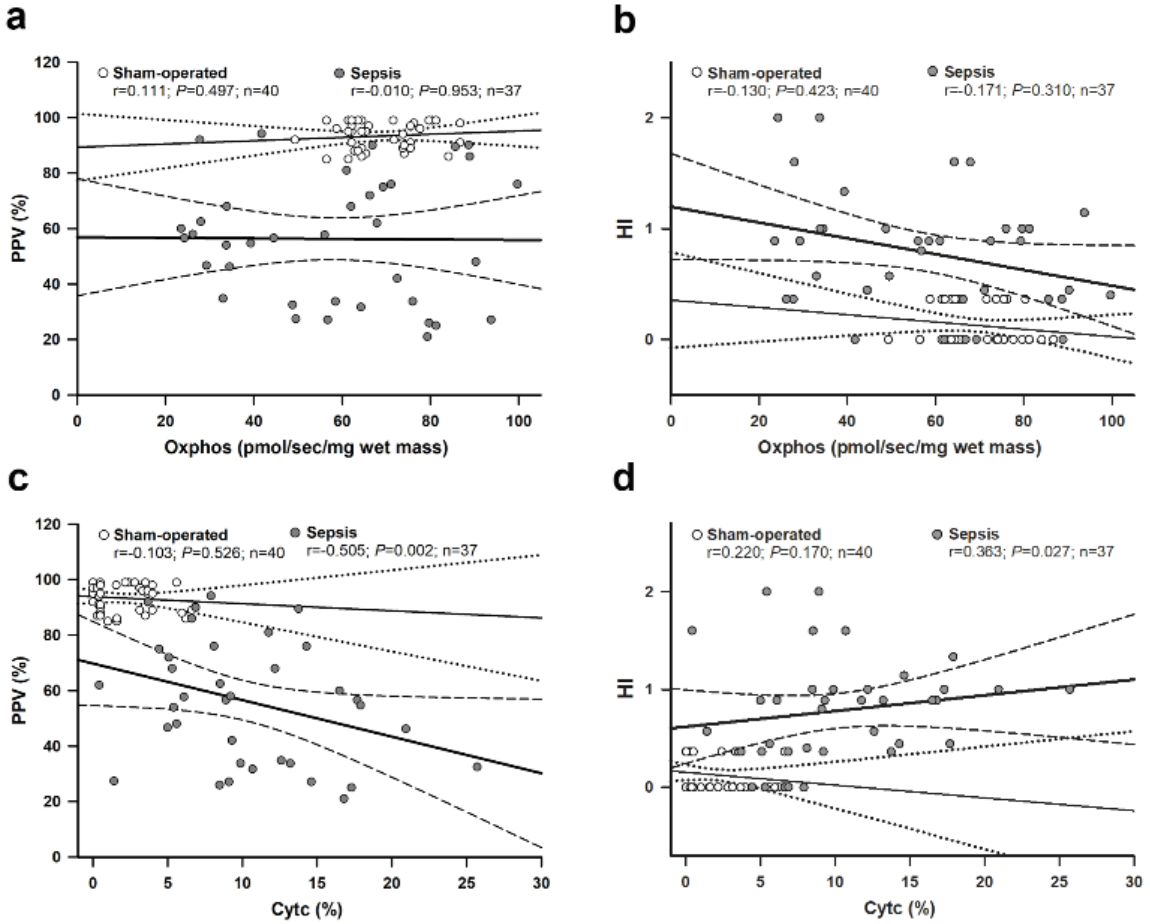

Figure 20. The correlation between oxidative phosphorylation (OxPhos) and **(a)** the proportion of perfused vessels (PPV) and **(b)** the heterogeneity index (HI) and between cytochrome c control efficiency (CytC%) and **(c)** PPV and **(d)** HI were examined with the Pearson correlation test. Correlation coefficient r values, (null hypothesis-related) *P* values and numbers of animals involved in the sham-operated and septic groups are provided with a 95% confidence interval. The sham-operated subgroup is marked with open circles, a thin regression line, and a dotted line for the 95% confidence interval, whereas the septic subgroup is indicated with dark gray circles, a thick regression line, and a dashed line for the 95% confidence interval.

5. Discussion

5.1. The impact of the microbial composition of inocula on sepsis progression

Several preclinical animal models of human sepsis with various advantages and disadvantages have already been presented to the scientific community (Poli-de-Figueiredo et al. 2008; Liu et al. 2016). In general terms, CLP is considered the most effective investigative tool; nevertheless, precise control of intestinal leakage is usually impossible (Dejager et al. 2011). Fecal inductions with standardized CFU concentration ranges are considered a suitable alternative (Garrido et al. 2004). In our hands, 1.02×10^6–5.6×10^6 CFUs correlated well with the onset time of severe reactions 24h later. This CFU range resulted in approx. 20% total mortality, broadly reproducing the 17–29% mortality rate of human intraabdominal sepsis (Claridge et al. 2014; Bauer et al. 2020). Here it should be noted that 24h for rats corresponds to a time interval of approx. 21 days in humans, due to the often overlooked 1:21 conversion ratio of the rat-human age correlation (Sengupta et al. 2013). The changes in signs and symptoms were further followed up to 72h; visible and measurable parameters were monitored and recorded sequentially, corresponding again to clinical practice. This approach demonstrated the resolution phase; the compensatory mechanisms led to recovery in the surviving cohort of animals between 24 and 72h.

Approximately 60% of human septic cases are caused by bacterial infections, and Gram-positive species are detected in the hemoculture in 46% of cases (Mayr et al. 2014). Monobacterial origin is rare in human sepsis. The literature agrees that E. coli is one of the most common pathogens, and, although the respiratory tract is the most frequent source of infection, abdominal origin also makes up a significant percentage (Dolin et al. 2019; Alberti et al. 2002). It should be noted that the flora of fecal peritonitis is generally considered polymicrobial. Still, the identification of endogenous or exogenous microbial sources is usually lacking in the design of animal model strategies. E. coli showed the highest frequency among the sepsis-causing bacteria we isolated (followed by Klebsiella, Pseudomonas, and Acinetobacter), a finding which is consistent with clinical experience (Dolin et al. 2019). However, sepsis with a Gram-positive source in rodents is relatively rare in contrast to the frequent occurrence of *Staphylococcus aureus* in human sepsis (Poli-de-Figueiredo et al. 2008).

Here we have demonstrated the paramount importance of identifying inducer strains because approx. 20% of the fecal solutions with a presumed polymicrobial habitat proved to be monomicrobial (with only E. coli present). Moreover, the monomicrobial induction was attributed exclusively to the 24h mortality, and the general condition of the hosts was more

severely impaired in these cases. This finding supports the view that E. coli may be responsible for early mortality in intraabdominal sepsis (Shah et al. 2016) but partially contradicts other results, where polymicrobial infections had a higher mortality rate (Aliaga et al. 2000). According to clinical studies, the progression depends mainly on the pathogen and on the clinicopathologic characteristics of the examined patient population (Aliaga et al. 2000; Marra et al. 2005; Zorgani et al. 2010; Wang et al. 2020). Karakonstantis et al. concluded in their meta-analysis that polybacterial sepsis has a lower mortality rate; however, the study had a high risk of bias, and we still have weak clinical evidence in this regard (Karakonstantis et al. 2021).

5.2. Temporal changes in the composition of the bacterial content during sepsis progression

It should be underlined that a shift from polymicrobial to monomicrobial content had begun during the preparation of the uniformly prepared and mixed stool samples and that the transition was then tracked within the animals' bodies. Another distinctive feature of the process was the Lactobacillus and Bifidobacteria cultures detected in the ascites perhaps as a compensatory sign of the host's bacterial defense mechanism (Liu et al. 2013). These strains exert anti-inflammatory effects and may enhance the stability of the intestinal barrier. Short-chain fatty acids, in particular acetate, propionate, and butyrate, are fermentation products of Lactobacilli and Bifidobacteria; they have a direct bactericidal effect by reducing intestinal pH and an immunomodulatory role by enhancing differentiation of regulatory T cells and stimulating the production of proinflammatory IL-10 (Smith et al. 2013). Butyrate reduces intestinal permeability by stabilizing the metabolism of the enterocytes and by enhancing the expression of tight junction proteins, such as occludin or claudin. Furthermore, these probiotic strains are thought to produce antimicrobial peptides and other organic acids that promote the elimination of pathogenic strains (Furusawa et al. 2013). These processes may explain the absence of mortality in the polymicrobial sepsis group in our experiments.

We followed the dynamics of the transition of bacterial strains in the surviving animals; the concentration and diversity of the polymicrobial cultures in the ascites decreased after 24h, and the most frequent strain was again E. coli (Barrera et al. 2011; Almeida et al. 2006; Priya and Blekhman 2019). However, new strains (e.g., *Neissera subflavia*) were also detected over time during the secondary peritonitis. Finally, the majority of the strains disappeared from the ascites, and only E. coli and *Lactobacillus murinus* were detected with reduced concentrations in the 72h samples. This observation may primarily be attributed to banal factors, such as the dramatic change of the bacterial habitat or unavoidable oxidative stress on anaerobic organisms.

However, it is important to highlight that strains that had previously not been observed also became detectable. The emergence of new species also raises the possibility of interaction between strains. Among these species, Lactobacilli are classified as probiotics and have special significance because they exert beneficial effects on the human body (Rossi et al. 2011; Williams 2010). Their presence is linked to the preservation of gut microbiota homeostasis and the initiation of anti-inflammatory processes, believed to be a result of the compounds they produce (O'Keefe 2008; O'Keefe et al. 2009). The exact processes underlying the higher survival rate observed after polymicrobial induction are not known, but bacteria-bacteria interaction may play an important role, resulting in the suppression of the strains responsible for fulminant progression (Sokol et al. 2008; Atarashi et al. 2011; Ivanov et al. 2009).

To our knowledge, our study is the first to demonstrate the dominant appearance of E. coli monomicrobial cultures in association with early mortality in experimental sepsis. A natural selection that is amplified under favorable conditions is the most likely explanation for the process (Russo et al. 1999; Mühldorfer and Hacker 1994) leading to microbial fitness and the "survival of the meanest" phenomenon. It should be noted that the results do not contradict MQTiPSS recommendations, as polymicrobial induction reflects the development of human sepsis better compared to monomicrobial inoculation (Garrido et al. 2004); however, besides dose responses, there is an obvious need for additional microbial tests to identify the dynamics of microbial changes.

5.3. The possible contribution of microcirculatory and mitochondrial changes to the severity of organ dysfunction in experimental sepsis

Study 2 was designed and ultimately proved to be sufficient to complement the results of Study 1 by examining the question from the perspective of clinical translatability: the changes of MMD components and their association with the MOF as a function of time. The model meets reproducibility criteria and offers similarity to a realistic clinical scenario with no source control (Brealey et al. 2004; Bauer et al. 2020; Tallósy et al. 2021; Fejes et al. 2024).

Our study presents a hypodynamic model of septic shock since CO dropped below the level of the sham-operated group while the increase in CO was only observed at 16h. Remarkably, the impaired intestinal serum microcirculation persisted from the start of the study despite the simultaneous increase in ExO_2, thus potentially indicating sustained cellular metabolic activity. Compared with other findings in the literature, our results are consistent with increased capillary O_2 extraction in early sepsis and emphasize microcirculatory dysfunction as

a central component of compromised DO_2 (Ellis et al. 2002). Recent studies also confirm microvascular dysfunction preceding detectable tissue damage (Kowalewska et al. 2022).

In this set-up, the divergent dynamics of sepsis-induced microcirculatory and mitochondrial responses were discerned with the presence of the whole septic macrohemodynamic pattern with compensatory hyperdynamic, decompensated hypodynamic, and final recovery stages, thus providing insight into the progression of sepsis without resuscitation. The joint feature of microcirculatory-mitochondrial impairment, or MMD, has already been identified as a significant element in the pathogenesis of human MOF (Brealey et al. 2002), but alterations to intestinal microcirculation and hepatic mitochondrial functions to date have not been studied together in MOF associated with intraabdominal sepsis (Clark and Coopersmith 2007; Nakajima et al. 2001; Andersson et al. 2012). In theory, a septic insult can affect all of the components of a microcirculatory system, and an increased capillary leakage, glycocalyx damage, or intravascular abnormalities can all lead to reduced oxygen diffusion and DO_2 within the affected tissues (Mammen 1998; Iba and Levy 2020; Spronk et al. 2004; Sullivan et al. 2021; László et al. 2021). Our study partially confirms this notion, showing an early proportionate decrease of perfused microvessels and increased perfusion heterogeneity with matching changes in ROFA scores. Nevertheless, the initial microcirculatory failure was improved and then restored in the later phase of the 28h observation period. Importantly, the hepatic mitochondrial function deteriorated much later with a rapid recovery of oxidation-linked parameters and a permanently sufficient coupling of the respiratory chain, but CytC% was elevated significantly, implying mitochondrial outer membrane (mtOM) damage. CytC is an electron shuttle protein loosely anchored to the mitochondrial inner membrane. Injury to mtOM leads to the partial loss of intramitochondrial CytC and decreased mitochondrial VO_2 (Borutaite et al. 2001; Andersen et al. 2016; Adachi et al. 2004). We have used an established respirometry method to determine mtOM integrity with stimulation of mitochondrial respiration following CytC replacement from an outer source (Kay et al. 1997; Eleftheriadis et al. 2006). In theory, damage to the mtOM should also involve impairment of mitochondrial coupling, but this was not the case here. CytC% had a high diagnostic power during the whole course of the 28h experimental period, thus suggesting that it may be a suitable biomarker for the onset of severe sepsis. However, despite this correlation, mtOM damage or OxPhos changes did not influence the ROFA score. Our results are consistent with the literature in terms of septic mtOM damage and deterioration of oxidative functions of the respiratory chain (Eyenga et al. 2022). However, the markedly rapid restoration of OxPhos suggests an immense reserve

capacity of hepatic mitochondrial respiration to compensate for the loss of membrane integrity. Of note, the correlation between ROFA scores and microcirculatory parameters indicates that the onset of MOF is mainly influenced by microvascular factors, and the correlation between microcirculatory variables and mtOM damage without the involvement of transient loss of oxidative capacities further confirms the presence of strong mitochondrial coping mechanisms against membrane damage.

Mitochondrial dysfunction can occur in sepsis both with and without shock as well, but it is not uniformly present. The pathogenesis is complex and still only partially known, but it seems that different mitochondrial functionalities may be present in adjacent areas with microvascular flow heterogeneity (Ince and Mik 2016). The non-uniformity may also result from the heterogeneous ultrastructural, biophysical, and electrochemical characteristics of liver mitochondria, which may lead to potentially decaying and surviving subpopulations in response to pathologies and post-translational processes (Ngo et al. 2021). Heterogeneity may also arise from the mitochondrial life cycle itself, including biogenesis, motility, fusion and fission, and the clearance of damaged mitochondria. In this line, damaged mitochondria can fuse with other mitochondria with intact membranes, and a regenerative fusion-fission phenomenon was already observed during sepsis progression. Thus, we hypothesize that increased CytC efflux – hypothetically expected from the increased membrane permeability – preceded the complete clearance of degraded mitochondria with mtOM damage and that a structurally and metabolically more resilient and compensatory subpopulation was able to maintain undisturbed ATP synthesis. These mitochondria may be maintainers or restorers of microcirculation and tissue integrity in the later period where sepsis is resolved (Chen et al. 2005).

In this study design, the ROFA score was used to monitor MOF progression similarly to the human clinical routine, and it was possible to establish the diagnostic value of the microcirculatory parameters within this scheme. As with human practice, the serum lactate level was also significantly elevated and proved to be a strong predictor of severity, supporting the diagnostic importance of hypoxia markers (Zhai et al. 2018). However, the low serum level of renal and hepatic dysfunction markers point to the direction of “septic stunning,” suggesting that the organs were primed with “hypoxic hibernation” for the expected insult.

Brealey et al. (2004) have described marked changes in mitochondrial functions, but microcirculation and MOF have not yet been detected simultaneously. We aimed to complement this lack of knowledge by using the latest consensus recommendations, a standardized MOF severity score system, and simultaneous microcirculatory measurements. Our experimental

protocol provided an opportunity to address the chicken or egg causality dilemma of MMD in sepsis. Microcirculation is a significantly earlier predictor of MOF as compared to mitochondrial respiration. We have used particular parameters to demonstrate that detectable microcirculatory or mitochondrial functional deteriorations occur at different time points depending on the course of sepsis and the compensatory mechanisms and that inappropriate monitoring times may lead to erroneous conclusions. By sequentially tracking the development of MOF, our results shed light on the dynamics of the microvascular oxygen supply, thus providing a better chance for the appropriate timing of diagnostic and therapeutic efforts (Figure 21).

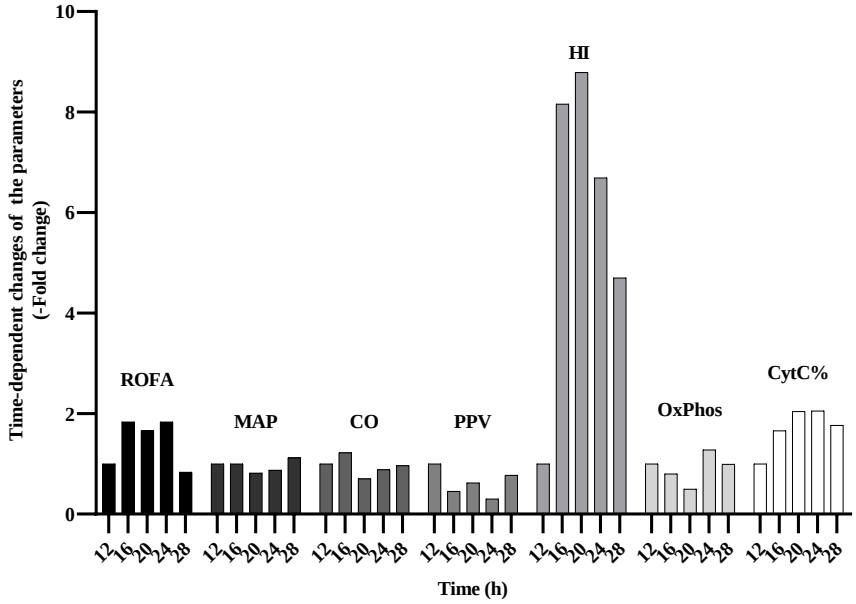

Figure 21. Rate of increase of different parameters over the study period compared to the 12h values in Study 2. Fold changes of ROFA score, mean arterial pressure (MAP), cardiac output (CO), proportion of perfused vessels (PPV), heterogeneity index (HI), oxidative phosphorylation (OxPhos), and cytochrome c control efficiency (CytC%) in the septic animals.

The results demonstrate that an early, marked microcirculatory dysfunction was followed by late (and presumably compensatory) mitochondrial changes during this time. The conventional abbreviation MMD with two capital Ms suggests an equivalent proportion in the pathogenesis of MOF and sepsis severity for both M components, but the microcirculatory arm of this process is much stronger. In light of the relevant scientific literature, it seems this finding is not unique. For this reason, the use of capital M should only represent the predominance of microcirculation and thus the abbreviation should be changed to MmD to indicate the disparity between the microcirculatory and mitochondrial components of the syndrome.

Although our study design did not include direct structural mitochondrial observations (e.g., microscopic detection of outer membrane damage) and thus some of our conclusions are based on the literature, we believe that our results have brought us closer to understanding the pathophysiology of septic MOF. By expanding the experimental toolbox and methodology, more sophisticated detection of pathophysiological changes may be possible in future experiments. Understanding the underlying processes of sepsis will not only contribute to a better understanding of the (patho)physiology of the microcirculatory-mitochondrial functional system but could also lead to significant diagnostic and therapeutic breakthroughs in human clinical practice.

5.4. Limitations

Our work contained some major limitations, which may warrant further investigation. In Study 1, the cross-sectional characterization reflected the most important features of the clinical disease, but extended monitoring may add further information. Further, the microbial identification time could be improved with novel methods, such as broad-range PCR amplification with high-resolution melt analysis (Hjelmsø et al. 2014). In Study 2, parallel microcirculation and mitochondrial study of the same organ would have been the perfect solution to test our hypothesis, but technical limitations (i.e., similar IDF signals of the liver parenchyma and red blood cells) precluded this possibility (Uz et al. 2020). It should be mentioned that due to the dominant portal blood supply of the liver, the incoming hypoxic signals from the intestines may influence hepatic mitochondrial functions. Meanwhile, respirometric evaluation of intestinal mitochondrial functions is highly limited due to the hindering effect of the high linolenic and oleic acid content, as these molecules can damage the mitochondrial membranes (Stanbury 1962). Furthermore, the complex structure of the intestinal wall and the potential spatial differences in mitochondrial behavior in the different histological layers could also have resulted in high variance of the data. A future experiment with the aim of separating the putative mitochondrial subpopulations structurally and functionally could best be investigated in isolated *in vitro* systems, which did not fit into the present experimental set-up. In both studies, only a population of healthy animals was evaluated without age and gender differences, and several other variables were not collected that have been demonstrated to influence bacterial reactions, such as diet composition. The points of the latest MQTiPSS recommendations should have been followed, but antibiotics were omitted from the protocol due to their incompletely mapped mitochondrial side-effects (Suárez-Rivero et al. 2021; Baráth et al. 2022). In terms of progression, a longer follow-up would have been preferable. Given the approx. 1:21 ratio of rat time–human time conversion, we can assume that the acute phase was fully covered (Sengupta et al. 2013), but additional studies are needed to explore the subsequent effects in later phases of sepsis.

6. New findings

1) We have optimized a rat model of fecal inoculation-induced, intraabdominal sepsis in terms of bacterial cell number and incubation time.

2) Our data indicate that the type of inducing and colonizing bacteria in the peritoneal sac significantly influence the outcome. This indicates the need for microbiological analysis when constructing a model of sepsis.

3) The results suggest the presence of competitive intraperitoneal bacterial processes, leading to an increased relative prevalence of certain dominant strains. This may also explain the development of varying sepsis severities.

4) The dynamic analysis of MMD, along with the deterioration of organ functions, demonstrated that these changes occur either in parallel with or as a potential pathophysiological basis for this process. In this context, it should be noted that ileal microvascular perfusion failure occurs earlier and has a higher predictive value for septic MOF than hepatic mitochondrial functional changes. These findings offer valuable translational insights, as they reflect mechanisms that may also be relevant in human sepsis pathophysiology.

5) Hepatic oxidative mitochondrial functions recover relatively rapidly, thus potentially indicating the existence of mitochondrial subpopulations with different responses to tissue hypoxia.

7. Funding

The work and publications were supported by the NKFIH K116689, GINOP-2.3.2-15-2016-00034, GINOP-2.3.2-15-2016-00015, and EFOP-3.6.2-16-2017-00006 grants. This research was conducted with the support of the Szeged Scientists Academy Program within the Foundation for the Future of Biomedical Sciences in Szeged under the sponsorship of the Hungarian Ministry of Human Capacities (EMMI:13725-2/2018/INTFIN).

8. Acknowledgements

I wish to convey my thanks to **Professor Mihály Boros**, the former head of the Institute of Surgical Research. I appreciate his encouragement and thank him for providing me the opportunity to start my scientific career at the Institute and carry out my research.

I am especially grateful to my supervisors and mentors, **József Kaszaki** and **Szabolcs Péter Tallósy**, for their guidance and support in helping me acquire experimental skills. They were tough and strict teachers but always fair and supportive. I was always able to rely on them for any kind of question during my work. Without their ongoing support, interest, and stimulating guidance, my doctoral thesis could hardly have come to fruition.

I am indebted to the **Szeged Scientists Academy Program**, which supported me between 2015 to 2021 and provided me with the opportunity to join the excellent team at the Institute of Surgical Research. The annual rigorous audits motivated me to consistently strive for successful and forward-thinking work.

Furthermore, I am grateful to the current and former staff in our research group, Andrea Szabó, **László Juhász, Attila Rutai, Marietta Zita Poles,** and **Liliána Kiss,** for their help and valuable work in improving the scientific value of the studies in this PhD thesis. I have to highlight the valuable guidance provided by **Andrea Szabó**. I greatly appreciate her generous help in the formulation of the publication of the Study 1 findings and during the work on my thesis.

I owe a debt of thanks to the **staff at the University of Szeged Department of Medical Microbiology Educational and Research Center** for their help and support with the qualitative and quantitative microbial measurements and to **Szabolcs Péter Tallósy** for being the link between the two institutes. Without their work, Study 1 would never have been conducted.

Above all, I wish to thank **my family, my mother, my father,** and **my other half** for their support and patience. Without them, I would never be able to achieve my goals.

9. References

Publications cited in the thesis are listed in alphabetical order according to the American Psychological Association (APA) style.

[1] Adachi, N., Kawakami, K., Matsuno, K., Miyamoto, K., Sato, C., & Yamana, H. (2004). Serum cytochrome c level as a prognostic indicator in patients with systemic inflammatory response syndrome. *Clinica Chimica Acta*, 342(1-2), 127-136.

[2] Aird, W. C. (2004). Endothelium as an organ system. *Critical Care Medicine*, 32(Supplement), S271-S279. https://doi.org/10.1097/01.CCM.0000131666.84812.5F

[3] Alberti, C., Brun-Buisson, C., Burchardi, H., Martin, C., Goodman, S., Artigas, A., Sicignano, A., Palazzo, M., Moreno, R., Boulmé, R., Lepage, E., & Le Gall, J. R. (2002). Epidemiology of sepsis and infection in ICU patients from an international multicenter cohort study. *Intensive Care Medicine*, 28(2), 108–121.

[4] Aliaga, L., Mediavilla, J. D., Llosá, J., Miranda, C., & Rosa-Fraile, M. (2000). Clinical significance of polymicrobial versus monomicrobial bacteremia involving Pseudomonas aeruginosa. *European Journal of Clinical Microbiology & Infectious Diseases*, 19(11), 871–874. https://doi.org/10.1007/s100960000392

[5] Almeida, J., Galhenage, S., Yu, J., Kurtovic, J., & Riordan, S. M. (2006). Gut flora and bacterial translocation in chronic liver disease. *World Journal of Gastroenterology*, 12(10), 1493.

[6] American College of Chest Physicians/Society of Critical Care Medicine Consensus Conference. (1992). Definitions for sepsis and organ failure and guidelines for the use of innovative therapies in sepsis. *Critical Care Medicine*, 20(6), 864-874.

[7] Andersen, L. W., Baek, L., Dreyer, P., Lange, T., & Bestle, M. H. (2016). Cytochrome C in patients with septic shock. *Shock*, 45(5), 512-517.

[8] Andersson, A., Fenyo, Z., & Wigenstam, E. (2012). Gut microcirculatory and mitochondrial effects of hyperdynamic endotoxaemic shock and norepinephrine treatment. *British Journal of Anaesthesia*, 108(2), 254-261.

[9] Arina, P., & Singer, M. (2021). Pathophysiology of sepsis. *Current Opinion in Anaesthesiology*, 34(2), 77–84.

[10] Armstrong, B. A., Betzold, R. D., & May, A. K. (2017). Sepsis and septic shock strategies. *Surgical Clinics of North America*, 97(6), 1339-1379. https://doi.org/10.1016/j.suc.2017.07.003

[11] Atarashi, K., Tanoue, T., Shima, T., Imaoka, A., Kuwahara, T., Momose, Y., Cheng, G., Yamasaki, S., Saito, T., Ohba, Y., Taniguchi, T., & Honda, K. (2011). Induction of colonic regulatory T cells by indigenous Clostridium species. *Science*, 331(6015), 337–341. https://doi.org/10.1126/science.1198469

[12] Aykut, G., Veenstra, G., Scorcella, C., Ince, C., & Boerma, C. (2015). Cytocam-IDF (incident dark field illumination) imaging for bedside monitoring of the microcirculation. *Intensive Care Medicine Experimental*, 3, 40. https://doi.org/10.1186/s40635-015-0040-7

[13] Baráth, B., Jász, D. K., Horváth, T., Baráth, B., Maróti, G., Strifler, G., Varga, G., Sándor, L., Perényi, D., Tallósy, S., ... & Köles, Z. (2022). Mitochondrial side effects of surgical prophylactic antibiotics ceftriaxone and rifaximin lead to bowel mucosal damage. *International Journal of Molecular Sciences*, *23*(9), 5064. https://doi.org/10.3390/ijms23095064

[14] Barrera, G., Pizarro, C., & Martinez, E. (2011). Model of polymicrobial peritonitis that induces the proinflammatory and immunosuppressive phases of sepsis. *Infection and Immunity*, 79(3), 1280–1288.

[15] Bauer, M., Gerlach, H., Vogelmann, T., Preissing, F., Stiefel, J., & Adam, D. (2020). Mortality in sepsis and septic shock in Europe, North America and Australia between 2009 and 2019: Results from a systematic review and meta-analysis. *Critical Care*, 24(1), 239. https://doi.org/10.1186/s13054-020-02950-2

[16] Bianchi, M. E. (2007). DAMPs, PAMPs and alarmins: All we need to know about danger. *Journal of Leukocyte Biology*, 81(1), 1-5.

[17] Bone, R. C., Balk, R. A., Cerra, F. B., Dellinger, R. P., Fein, A. M., Knaus, W. A., & others. (1992). Definitions for sepsis and organ failure and guidelines for the use of innovative therapies in sepsis. *Chest*, 101(6), 1644–1655. https://doi.org/10.1378/chest.101.6.1644

[18] Bone, R. C., Fisher, C. J. Jr., Clemmer, T. P., Slotman, G. J., Metz, C. A., & Balk, R. A. (1987). A controlled clinical trial of high-dose methylprednisolone in the treatment of severe sepsis and septic shock. *New England Journal of Medicine*, 317(11), 653-658. https://doi.org/10.1056/NEJM198709103171101

[19] Bone, R. C., Fisher, C. J. Jr., Clemmer, T. P., Slotman, G. J., Metz, C. A., & Balk, R. A. (1989). Sepsis syndrome: A valid clinical entity. *Critical Care Medicine*, 17(5), 389-393.

[20] Borutaite, V., Budriunaite, A., Morkuniene, R., & Brown, G. C. (2001). Release of mitochondrial cytochrome c and activation of cytosolic caspases induced by myocardial ischaemia. *Biochimica et Biophysica Acta*, 1537(1), 101-109.

[21] Brand, M. D. (2016). Mitochondrial generation of superoxide and hydrogen peroxide as the source of mitochondrial redox signaling. *Free Radical Biology and Medicine*, 100, 14-31. https://doi.org/10.1016/j.freeradbiomed.2016.04.001

[22] Brealey, D., Brand, M. D., & Hargreaves, I. (2002). Association between mitochondrial dysfunction and severity and outcome of septic shock. *The Lancet*, 360(9328), 219-223.

[23] Brealey, D., Karyampudi, S., & Hargreaves, I. (2004). Mitochondrial dysfunction in a long-term rodent model of sepsis and organ failure. *American Journal of Physiology - Regulatory, Integrative and Comparative Physiology*, 286(3), 491-497.

[24] Buras, J. A., Holzmann, B., & Sitkovsky, M. (2005). Animal models of sepsis: Setting the stage. *Nature Reviews Drug Discovery*, 4(10), 854-865. https://doi.org/10.1038/nrd1854

[25] Cabrera-Perez, J., Badovinac, V. P., & Griffith, T. S. (2017). Enteric immunity, the gut microbiome, and sepsis: Rethinking the germ theory of disease. *Experimental Biology and Medicine*, 242(2), 127–139. https://doi.org/10.1177/1535370216669610

[26] Cai, L., Rodgers, E., Schoenmann, N., & Raju, R. P. (2023). Advances in rodent experimental models of sepsis. *International Journal of Molecular Sciences*, 24(11), 9578. https://doi.org/10.3390/ijms24119578

[27] Chen, H., Chomyn, A., & Chan, D. C. (2005). Disruption of fusion results in mitochondrial heterogeneity and dysfunction. *Journal of Biological Chemistry*, 280(30), 26185–26192. https://doi.org/10.1074/jbc.M501881200

[28] Claridge, J. A., & McMahon, R. (2014). Bacterial species-specific hospital mortality rate for intra-abdominal infections. *Surgical Infections (Larchmt)*, 15(2), 194–199. https://doi.org/10.1089/sur.2012.181

[29] Clark, J. A., & Coopersmith, C. M. (2007). Intestinal crosstalk: A new paradigm for understanding the gut as the "motor" of critical illness. *Shock*, 28(4), 384-393. https://doi.org/10.1097/shk.0b013e318149089d

[30] Clowes, G. H., O'Donelli, T. F., & Ryan, N. T. (1974). Energy metabolism in sepsis: Treatment based on different patterns in shock and high output stage. *Annals of Surgery*, 179(6), 684–694. https://doi.org/10.1097/00000658-197406000-00006

[31] Coopersmith, C. M., De Backer, D., Deutschman, C. S., Ferrer, R., Lat, I., Machado, F. R., Martin, G. S., Martin-Loeches, I., Nunnally, M. E., Antonelli, M., Evans, L. E., Hellman, J., Jog, S., Kesecioglu, J., Levy, M. M., & Rhodes, A. (2018). Surviving Sepsis Campaign:

Research priorities for sepsis and septic shock. *Critical Care Medicine*, 46(8), 1334-1356. https://doi.org/10.1097/CCM.0000000000003225

[32] De Backer, D., Creteur, J., Preiser, J. C., Dubois, M. J., & Vincent, J. L. (2002). Microvascular blood flow is altered in patients with sepsis. *American Journal of Respiratory and Critical Care Medicine*, 166(1), 98-104. https://doi.org/10.1164/rccm.200111-1352OC

[33] De Backer, D., Donadello, K., Sakr, Y., & et al. (2013). Microcirculatory alterations in patients with severe sepsis: Impact of time of assessment and relationship with outcome. *Critical Care Medicine*, 41(4), 791–799. https://doi.org/10.1097/CCM.0b013e31827e3b8b

[34] Dejager, L., Pinheiro, I., Dejonckheere, E., & Libert, C. (2011). Cecal ligation and puncture: The gold standard model for polymicrobial sepsis? *Trends in Microbiology*, 19(4), 198-208. https://doi.org/10.1016/j.tim.2011.01.001

[35] Dellinger, R. P., Carlet, J. M., Masur, H., Gerlach, H., Calandra, T., Cohen, J., & others. (2004). Surviving Sepsis Campaign guidelines for the management of severe sepsis and septic shock. *Critical Care Medicine*, 32(3), 858–873. https://doi.org/10.1097/01.CCM.0000117317.18092.E4

[36] Dolin, H. H., Papadimos, T. J., Chen, X., & Pan, Z. K. (2019). Characterization of pathogenic sepsis etiologies and patient profiles: A novel approach to triage and treatment. *Microbiology Insights*, 12, 1178636118825081. https://doi.org/10.1177/1178636118825081

[37] Donati, A., Domizi, R., Damiani, E., Adrario, E., Pelaia, P., & Ince, C. (2013). From macrohemodynamic to the microcirculation. *Critical Care Research and Practice*, 2013, 892710. https://doi.org/10.1155/2013/892710

[38] Edul, V. S., Enrico, C., Laviolle, B., Vazquez, A. R., Ince, C., & Dubin, A. (2012). Quantitative assessment of the microcirculation in healthy volunteers and in patients with septic shock. *Critical Care Medicine*, 40(5), 1443-1448. https://doi.org/10.1097/CCM.0b013e31823dae59

[39] Eleftheriadis, T., Pissas, G., Liakopoulos, V., & Stefanidis, I. (2016). Cytochrome c as a potentially clinically useful marker of mitochondrial and cellular damage. *Frontiers in Immunology*, 7, 279. https://doi.org/10.3389/fimmu.2016.00279

[40] Ellis, C. G., Bateman, R. M., Sharpe, M. D., Sibbald, W. J., & Gill, R. (2002). Effect of a maldistribution of microvascular blood flow on capillary O_2 extraction in sepsis. *American Journal of Physiology - Heart and Circulatory Physiology*, 282(1), 156-164. https://doi.org/10.1152/ajpheart.2002.282.1.156

[41] Eyenga, P., Rey, B., Eyenga, L., & Sheu, S. S. (2022). Regulation of oxidative phosphorylation of liver mitochondria in sepsis. *Cells*, 11(10), 1598. https://doi.org/10.3390/cells11101598

[42] Furusawa, Y., Obata, Y., Fukuda, S., Endo, T. A., Nakato, G., Takahashi, D., ... & Ohno, H. (2013). Commensal microbe-derived butyrate induces the differentiation of colonic regulatory T cells. *Nature, 504*(7480), 446-450. https://doi.org/10.1038/nature12721

[43] Garrido, A. G., de Figueiredo, L. F. P., & Silva, M. R. E. (2004). Experimental models of sepsis and septic shock: An overview. *Acta Cirúrgica Brasileira*, 19(2), 82–88. https://doi.org/10.1590/S0102-86502004000200001

[44] Hernandez, G., Bruhn, A., & Ince, C. (2013). Microcirculation in sepsis: New perspectives. *Current Vascular Pharmacology*, 11(2), 161-169. https://doi.org/10.2174/157016113805530024

[45] Hjelmsø, M. H., et al. (2014). High-resolution melt analysis for rapid comparison of bacterial community compositions. *Applied and Environmental Microbiology*, 80(11), 3568-3575. https://doi.org/10.1128/AEM.03923-13

[46] Iba, T., & Levy, J. H. (2020). Sepsis-induced coagulopathy and disseminated intravascular coagulation. *Anesthesiology*, 132(6), 1238-1245. https://doi.org/10.1097/ALN.0000000000003216

[47] Idelevich, E. A., Schüle, I., Grünastel, B., Wüllenweber, J., Peters, G., & Becker, K. (2014). Rapid identification of microorganisms from positive blood cultures by MALDI-TOF mass spectrometry subsequent to very short-term incubation on solid medium. *Clinical Microbiology and Infection*, 20(10), 1001-1006. https://doi.org/10.1111/1469-0691.12640

[48] Ince, C. (2005). The microcirculation is the motor of sepsis. *Critical Care*, 9(Suppl 4), S13-S19. https://doi.org/10.1186/cc3753

[49] Ince, C., & Sinaasappel, M. (1999). Microcirculatory oxygenation and shunting in sepsis and shock. *Critical Care Medicine*, 27(7), 1369-1377. https://doi.org/10.1097/00003246-199907000-00018

[50] Ince, C., Boerma, E. C., Cecconi, M., & et al. (2018). Second consensus on the assessment of sublingual microcirculation in critically ill patients: Results from a task force of the European Society of Intensive Care Medicine. *Intensive Care Medicine*, 44(3), 281-299. https://doi.org/10.1007/s00134-017-5086-4

[51] Ivanov, I. I., Atarashi, K., Manel, N., Brodie, E. L., Shima, T., Karaoz, U., Wei, D., Goldfarb, K. C., Santee, C. A., Lynch, S. V., & et al. (2009). Induction of intestinal Th17 cells by segmented filamentous bacteria. *Cell*, 139(3), 485–498. https://doi.org/10.1016/j.cell.2009.09.033

[52] Jackson, S. J., Andrews, N., Ball, D., Bellantuono, I., Gray, J., Hachoumi, L., Holmes, A., Latcham, J., Petrie, A., Potter, P., Rice, A., Ritchie, A., Stewart, M., Strepka, C., Yeoman, M., & Chapman, K. (2017). Does age matter? The impact of rodent age on study outcomes. *Laboratory Animals*, 51(2), 160-169. https://doi.org/10.1177/0023677216653984

[53] Jastroch, M., Divakaruni, A. S., Mookerjee, S., Treberg, J. R., & Brand, M. D. (2010). Mitochondrial proton and electron leaks. *Essays in Biochemistry*, 47, 53-67. https://doi.org/10.1042/bse0470053

[54] Juhász, L., Rutai, A., Fejes, R., Tallósy, S. P., Poles, M. Z., Szabó, A., Szatmári, I., Fülöp, F., Vécsei, L., Boros, M., & Kaszaki, J. (2020). Divergent effects of the N-methyl-D-aspartate receptor antagonist kynurenic acid and the synthetic analog SZR-72 on microcirculatory and mitochondrial dysfunction in experimental sepsis. *Frontiers in Medicine*, 7, 566582. https://doi.org/10.3389/fmed.2020.566582

[55] Karakonstantis, S., & Kritsotakis, E. I. (2021). Systematic review and meta-analysis of the proportion and associated mortality of polymicrobial (vs monomicrobial) pulmonary and bloodstream infections by *Acinetobacter baumannii* complex. *Infection*, 49(6), 1149-1161. https://doi.org/10.1007/s15010-021-01663-0

[56] Kay, L., Daneshrad, Z., & Saks, V. A. (1997). Alteration in the control of mitochondrial respiration by outer mitochondrial membrane and creatine during heart preservation. *Cardiovascular Research*, 34(4), 547-556. https://doi.org/10.1016/S0008-6363(97)00183-6

[57] Kowalewska, P. M., & et al. (2022). Spectroscopy detects skeletal muscle microvascular dysfunction during onset of sepsis in a rat fecal peritonitis model. *Scientific Reports*, 12, 6339. https://doi.org/10.1038/s41598-022-10208-w

[58] Kreymann, G., Grosser, S., Buggisch, P., Gottschall, C., Matthaei, S., & Greten, H. (1993). Oxygen consumption and resting metabolic rate in sepsis, sepsis syndrome, and septic shock. *Critical Care Medicine*, 21(7), 1012-1019.

[59] Lam, C., Tyml, K., Martin, C., & Sibbald, W. J. (1994). Microvascular perfusion is impaired in a rat model of normotensive sepsis. *Journal of Clinical Investigation*, 94(5), 2077-2083. https://doi.org/10.1172/JCI117847

[60] Lamkanfi, M., & Dixit, V. M. (2014). Mechanisms and functions of inflammasomes. *Cell*, 157(5), 1013-1022. https://doi.org/10.1016/j.cell.2014.04.007

[61] Lang, C. H., Bagby, G. J., Ferguson, J. L., & Spritzer, J. J. (1984). Cardiac output and redistribution of organ blood flow in hypermetabolic sepsis. *American Journal of Physiology*, 246(3), 331-337.

[62] László, I., Csákány, L., Veres, A., Németh, M., Poles, M. Z., Kaszaki, J., Molnár, Z., & Szabó, A. (2021). Az endotheliális glycocalyx megjelenítése és vastagságának meghatározása intravitális mikroszkópiával [Visualization and determination of the endothelial glycocalyx thickness using intravital microscopy]. *Aneszteziológia és Intenzív Terápia*, 51(4), 11-20.

[63] Lewis, A. J., Billiar, T. R., & Rosengart, M. R. (2016). Biology and metabolism of sepsis: Innate immunity, bioenergetics, and autophagy. *Surgical Infections*, 17(3), 286-293. https://doi.org/10.1089/sur.2015.262

[64] Lidington, D., Ouellette, Y., Li, F., & Tyml, K. (2003). Conducted vasoconstriction is reduced in a mouse model of sepsis. *Journal of Vascular Research*, 40(2), 149-158. https://doi.org/10.1159/000069410

[65] Liu, D. Q., Gao, Q. Y., Liu, H. B., Li, D. H., & Wu, S. W. (2013). Probiotics improve survival of septic rats by suppressing conditioned pathogens in ascites. *World Journal of Gastroenterology*, 19(25), 4053-4059. https://doi.org/10.3748/wjg.v19.i25.4053

[66] Liu, D., Huang, S.-Y., Sun, J.-H., Zhang, H.-C., Cai, Q.-L., Gao, C., Li, L., Cao, J., Xu, F., Zhou, Y., & et al. (2022). Sepsis-induced immunosuppression: Mechanisms, diagnosis and current treatment options. *Military Medicine Research*, 9, 56. https://doi.org/10.1186/s40779-022-00392-5

[67] Liu, X., Wang, N., Wei, G., Fan, S., Lu, Y., Zhu, Y., Chen, Q., Huang, M., Zhou, H., & Zheng, J. (2016). Consistency and pathophysiological characterization of a rat polymicrobial sepsis model via the improved cecal ligation and puncture surgery. *International Immunopharmacology*, 32, 66-75. https://doi.org/10.1016/j.intimp.2015.12.041

[68] Mammen, E. F. (1998). The haematological manifestations of sepsis. *Journal of Antimicrobial Chemotherapy*, 41(1), 17-24. https://doi.org/10.1093/jac/41.1.17

[69] Marra, A. R., Bearman, G. M., Wenzel, R. P., & Edmond, M. B. (2005). Comparison of the systemic inflammatory response syndrome between monomicrobial and polymicrobial *Pseudomonas aeruginosa* nosocomial bloodstream infections. *BMC Infectious Diseases*, 5, 94. https://doi.org/10.1186/1471-2334-5-94

[70] Mayr, F. B., Yende, S., & Angus, D. C. (2014). Epidemiology of severe sepsis. *Virulence*, 5(1), 4–11. https://doi.org/10.4161/viru.27372

[71] Meng, L. (2021). Heterogeneous impact of hypotension on organ perfusion and outcomes: A narrative review. *British Journal of Anaesthesia*, 127(6), 845-861. https://doi.org/10.1016/j.bja.2021.06.048

[72] Merz, T., Denoix, N., Huber-Lang, M., Singer, M., Radermacher, P., & McCook, O. (2020). Microcirculation vs. mitochondria—What to target? *Frontiers in Medicine*, 7, 416. https://doi.org/10.3389/fmed.2020.00416

[73] Miranda, M. L., Balarini, M. M., & Bouskela, E. (2015). Dexmedetomidine attenuates the microcirculatory derangements evoked by experimental sepsis. *Anesthesiology*, 122(3), 619-630. https://doi.org/10.1097/ALN.0000000000000556

[74] Mühldorfer, I., & Hacker, J. (1994). Genetic aspects of *Escherichia coli* virulence. *Microbial Pathogenesis*, 16(3), 171–181. https://doi.org/10.1006/mpat.1994.1018

[75] Murando, F., Peloso, A., & Cobianchi, L. (2019). Experimental abdominal sepsis: Sticking to an awkward but still useful translational model. *Mediators of Inflammation*, 6, 1–8. https://doi.org/10.1155/2019/2829460

[76] Nagy, E., Becker, S., Kostrzewa, M., Barta, N., & Urbán, E. (2012). The value of MALDI-TOF MS for the identification of clinically relevant anaerobic bacteria in routine laboratories. *Journal of Medical Microbiology*, 61(9), 1393–1400. https://doi.org/10.1099/jmm.0.043474-0

[77] Nakajima, Y., Baudry, N., Duranteau, J., & Vicaut, E. (2001). Microcirculation in intestinal villi: A comparison between hemorrhagic and endotoxin shock. *American Journal of Respiratory and Critical Care Medicine*, 164(8), 2009–2016. https://doi.org/10.1164/ajrccm.164.8.2009065

[78] Nakamori, Y., Park, E. J., & Shimaoka, M. (2021). Immune deregulation in sepsis and septic shock: Reversing immune paralysis by targeting PD-1/PD-L1 pathway. *Frontiers in Immunology*, 11, 624279. https://doi.org/10.3389/fimmu.2020.624279

[79] Nandi, M., Jackson, S. K., Macrae, D., Shankar-Hari, M., Tremoleda, J. L., & Lilley, E. (2020). Rethinking animal models of sepsis - Working towards improved clinical translation whilst integrating the 3Rs. *Clinical Science*, 134(13), 1715-1734. https://doi.org/10.1042/CS20200679

[80] Nedel, W., Deutschendorf, C., & Portela, L. V. C. (2023). Sepsis-induced mitochondrial dysfunction: A narrative review. *World Journal of Critical Care Medicine*, 12(3), 139-152. https://doi.org/10.5492/wjccm.v12.i3.139

[81] Ngo, J., Osto, C., Villalobos, F., & Shirihai, O. S. (2021). Mitochondrial heterogeneity in metabolic diseases. *Biology*, 10(9), 927. https://doi.org/10.3390/biology10090927

[82] O'Keefe, S. J. (2008). Nutrition and colonic health: The critical role of the microbiota. *Current Opinion in Gastroenterology*, 24(1), 51-58. https://doi.org/10.1097/MOG.0b013e3282f2b7f2

[83] O'Keefe, S. J., Ou, J., Aufreiter, S., O'Connor, D., Sharma, S., Sepulveda, J., Fukuwatari, T., Shibata, K., & Mawhinney, T. (2009). Products of the colonic microbiota mediate the effects of diet on colon cancer risk. *The Journal of Nutrition*, 139(11), 2044-2048. https://doi.org/10.3945/jn.109.104380

[84] Osuchowski, M. F., Ayala, A., Bahrami, S., Bauer, M., Boros, M., Cavaillon, J. M., Chaudry, I. H., Coopersmith, C. M., Deutschman, C. S., Drechsler, S., Efron, P., Frostell, C., Fritsch, G., Gozdzik, W., Hellman, J., Huber-Lang, M., Inoue, S., Knapp, S., Kozlov, A. V., Libert, C., Zingarelli, B. (2018). Minimum Quality Threshold in Pre-Clinical Sepsis Studies (MQTiPSS): An International Expert Consensus Initiative for Improvement of Animal Modeling in Sepsis. *Shock (Augusta, Ga.)*, *50*(4), 377–380. https://doi.org/10.1097/SHK.0000000000001212

[85] Poli-de-Figueiredo, L. F., Garrido, A. G., Nakagawa, N., & Sannomiya, P. (2008). Experimental models of sepsis and their clinical relevance. *Shock*, 30(Suppl 1), 53-59. https://doi.org/10.1097/SHK.0b013e318181a343

[86] Pozo, M. O., Kanoore Edul, V. S., Ince, C., & Dubin, A. (2012). Comparison of different methods for the calculation of the microvascular flow index. *Critical Care Research and Practice*, 2012, 102483. https://doi.org/10.1155/2012/102483

[87] Preau, S., Vodovar, D., Jung, B., Lancel, S., Zafrani, L., Flatres, A., Oualha, M., Voiriot, G., Jouan, Y., Joffre, J., Uhel, F., De Prost, N., Silva, S., Azabou, E., & Radermacher, P. (2021). Energetic dysfunction in sepsis: A narrative review. *Annals of Intensive Care*, 11(1), 104. https://doi.org/10.1186/s13613-021-00893-7

[88] Priya, S., & Blekhman, R. (2019). Population dynamics of the human gut microbiome: Change is the only constant. *Genome Biology*, 20(1), 150. https://doi.org/10.1186/s13059-019-1816-0

[89] Protti, A., & Singer, M. (2006). Bench-to-bedside review: Potential strategies to protect or reverse mitochondrial dysfunction in sepsis-induced organ failure. *Critical Care*, 10(3), 228. https://doi.org/10.1186/cc4947

[90] Rossi, M., Amaretti, A., & Raimondi, S. (2011). Folate production by probiotic bacteria. *Nutrients*, 3(2), 118-134. https://doi.org/10.3390/nu3010118

[91] Russo, T. A., Carlino, U. B., Mong, A., & Jodush, S. T. (1999). Identification of genes in an extraintestinal isolate of *Escherichia coli* with increased expression after exposure to human urine. *Infection and Immunity*, 67(10), 5306-5314. https://doi.org/10.1128/IAI.67.10.5306-5314.1999

[92] Rutai, A., Fejes, R., Juhász, L., Tallósy, S. P., Poles, M. Z., Földesi, I., Mészáros, A. T., Szabó, A., Boros, M., & Kaszaki, J. (2020). Endothelin A and B receptors: Potential targets for microcirculatory-mitochondrial therapy in experimental sepsis. *Shock*, 54(1), 87-95. https://doi.org/10.1097/SHK.0000000000001414

[93] Rutai, A., Zsikai, B., Tallósy, S. P., Érces, D., Bizánc, L., Juhász, L., Poles, M. Z., Sóki, J., Baaity, Z., Fejes, R., Varga, G., Földesi, I., Burián, K., Szabó, A., Boros, M., & Kaszaki, J. (2022). A porcine sepsis model with numerical scoring for early prediction of severity. *Frontiers in Medicine*, 9, 867796. https://doi.org/10.3389/fmed.2022.867796

[94] Salomão, R., Ferreira, B. L., Salomão, M. C., Santos, S. S., Azevedo, L. C. P., & Brunialti, M. K. C. (2019). Sepsis: Evolving concepts and challenges. *Brazilian Journal of Medical and Biological Research*, 52(4), e8595. https://doi.org/10.1590/1414-431X20198595

[95] Sanders, E. R. (2012). Aseptic laboratory techniques: Plating methods. *Journal of Visualized Experiments*, (63), e3064. https://doi.org/10.3791/3064

[96] Sauer, S., Freiwald, A., Maier, T., Kube, M., Reinhardt, R., Kostrzewa, M., & Geider, K. (2008). Classification and identification of bacteria by mass spectrometry and computational analysis. *PLoS One*, 3(7), e2843. https://doi.org/10.1371/journal.pone.0002843

[97] Scheeren, T. W. L., & Ramsay, M. A. E. (2019). New developments in hemodynamic monitoring. *Journal of Cardiothoracic and Vascular Anesthesia*, 33(Suppl 1), S67-S72. https://doi.org/10.1053/j.jvca.2019.03.043

[98] Sengupta, P. (2013). The laboratory rat: Relating its age with human's. *International Journal of Preventive Medicine*, 4(6), 624-630. https://doi.org/10.4103/2008-7802.122436

[99] Shah, P. M., et al. (2016). Do polymicrobial intra-abdominal infections have worse outcomes than monomicrobial intra-abdominal infections? *Surgical Infections*, 17(1), 27-31. https://doi.org/10.1089/sur.2015.127

[100] Siegman-Igra, Y., Kulka, T., Schwartz, D., & Konforti, N. (1994). Polymicrobial and monomicrobial bacteraemic urinary tract infection. *Journal of Hospital Infection*, 28(1), 49-56. https://doi.org/10.1016/0195-6701(94)90152-x

[101] Singer, M., Deutschman, C. S., Seymour, C. W., Shankar-Hari, M., Annane, D., Bauer, M., Bellomo, R., Bernard, G. R., Chiche, J. D., Coopersmith, C. M., Hotchkiss, R. S., Levy, M. M., Marshall, J. C., Martin, G. S., Opal, S. M., Rubenfeld, G. D., van der Poll, T., Vincent, J. L., & Angus, D. C. (2016). The Third International Consensus Definitions for Sepsis and Septic Shock (Sepsis-3). *JAMA*, 315(8), 801-810. https://doi.org/10.1001/jama.2016.0287

[102] Smith, P. M., Howitt, M. R., Panikov, N., Michaud, M., Gallini, C. A., Bohlooly, Y. M., ... & Garrett, W. S. (2013). The microbial metabolites, short-chain fatty acids, regulate colonic Treg cell homeostasis. *Science, 341*(6145), 569-573. https://doi.org/10.1126/science.1241165

[103] Sokol, H., Pigneur, B., Watterlot, L., Lakhdari, O., Bermúdez-Humarán, L. G., Gratadoux, J. J., Blugeon, S., Bridonneau, C., Furet, J. P., Corthier, G., & et al. (2008). *Faecalibacterium prausnitzii* is an anti-inflammatory commensal bacterium identified by gut microbiota analysis of Crohn disease patients. *Proceedings of the National Academy of Sciences of the United States of America*, 105(43), 16731-16736. https://doi.org/10.1073/pnas.0804812105

[104] Soop, A., Albert, J., Weitzberg, E., Bengtsson, A., Lundberg, J. O. N., & Sollevi, A. (2004). Complement activation, endothelin-1 and neuropeptide Y in relation to the cardiovascular response to endotoxin-induced systemic inflammation in healthy volunteers. *Acta Anaesthesiologica Scandinavica*, 48(1), 74-81. https://doi.org/10.1111/j.1399-6576.2004.00390.x

[105] Spronk, P. E., Zandstra, D. F., & Ince, C. (2004). Bench-to-bedside review: Sepsis is a disease of the microcirculation. *Critical Care*, 8(6), 462-468. https://doi.org/10.1186/cc2957

[106] Stanbury, P. J. (1923). Comparison of the mitochondria of the small intestine of vertebrates. *Nature*, 192, 67.

[107] Suárez-Rivero, J. M., et al. (2021). Mitochondria and antibiotics: For good or for evil? *Biomolecules*, 11(7), 1050. https://doi.org/10.3390/biom11071050

[108] Sullivan, R. C., Rockstrom, M. D., Schmidt, E. P., & Hippensteel, J. A. (2021). Endothelial glycocalyx degradation during sepsis: Causes and consequences. *Matrix Biology Plus*, 12, 100094. https://doi.org/10.1016/j.mbplus.2021.100094

[109] Szabó, C. (2003). Multiple pathways of peroxynitrite cytotoxicity. *Toxicology Letters*, 140–141, 105-112. https://doi.org/10.1016/S0378-4274(02)00507-6

[110] Taeb, A. M., Hooper, M. H., & Marik, P. E. (2017). Sepsis: Current definition, pathophysiology, diagnosis, and management. *Nutrition in Clinical Practice*, 32(3), 296-308. https://doi.org/10.1177/0884533617695243

[111] Tallósy, S. P., Poles, M. Z., Rutai, A., Fejes, R., Juhász, L., Burián, K., Sóki, J., Szabó, A., Boros, M., & Kaszaki, J. (2021). The microbial composition of the initial insult can predict the prognosis of experimental sepsis. *Scientific Reports*, 11(1), 22772. https://doi.org/10.1038/s41598-021-02129-x

[112] Thiemermann, C., Wang, P., Wiersinga, W. J., & Xiao, Perret, C. (n.d.). L'hémodynamique au cours du choc septique [Hemodynamics during septic shock]. *Schweizerische Medizinische Wochenschrift*, 110(2), 56-61.

[113] Trásy, D., & Molnár, Z. (2023). A sepsis – közös ügyünk. *Magyar Belorvosi Archívum*, 76(4), 178-184. https://doi.org/10.59063/mba.2023.76.4.3

[114] Trzeciak, S., Cinel, I., Dellinger, R. P., Shapiro, N. I., Arnold, R. C., Parrillo, J. E., & Hollenberg, S. M. (2008). Resuscitating the microcirculation in sepsis: The central role of nitric oxide, emerging concepts for novel therapies, and challenges for clinical trials. *Academic Emergency Medicine*, 15(5), 399-413. https://doi.org/10.1111/j.1553-2712.2008.00068.x

[115] Tyagi, A., Sethi, A. K., Girotra, G., & Mohta, M. (2009). The microcirculation in sepsis. *Indian Journal of Anaesthesia*, 53(3), 281-293. https://doi.org/10.4103/0019-5049.53367

[116] Uz, Z., et al. (2020). Intraoperative imaging techniques to visualize hepatic (micro)perfusion: An overview. *European Surgical Research*, 61(1), 2-13. https://doi.org/10.1159/000508790

[117] Wang, Y. C., Ku, W. W., Yang, Y. S., Kao, C. C., Kang, F. Y., Kuo, S. C., Chiu, C. H., Chen, T. L., Wang, F. D., & Lee, A. Y. (2020). Is polymicrobial bacteremia an independent risk factor for mortality in *Acinetobacter baumannii* bacteremia? *Journal of Clinical Medicine*, 9(1), 153. https://doi.org/10.3390/jcm9010153

[118] Wiersinga, W. J., & van der Poll, T. (2022). Immunopathophysiology of human sepsis. *EBioMedicine*, 86, 104363. https://doi.org/10.1016/j.ebiom.2022.104363

[119] Wiersinga, W. J., Leopold, S. J., Cranendonk, D. R., & van der Poll, T. (2014). Host innate immune responses to sepsis. *Virulence*, 5(1), 36-44. https://doi.org/10.4161/viru.25436

[120] Wildner, G. (2019). Are rats more human than mice? *Immunobiology*, 224(1), 172-176. https://doi.org/10.1016/j.imbio.2018.09.002

[121] Williams, N. T. (2010). Probiotics. *American Journal of Health-System Pharmacy*, 67(6), 449-458. https://doi.org/10.2146/ajhp090379

[122] Zhai, X., et al. (2018). Lactate as a potential biomarker of sepsis in a rat cecal ligation and puncture model. *Mediators of Inflammation*, 2018, 8352727. https://doi.org/10.1155/2018/8352727

[123] Zorgani, A., Franka, R. A., Zaidi, M. M., Alshweref, U. M., & Elgmati, M. (2010). Trends in nosocomial bloodstream infections in a burn intensive care unit: An eight-year survey. *Annals of Burns and Fire Disasters*, 23(2), 88-94.

Disclosures

Co-author certification

I, myself as a corresponding author of the following publication(s) declare that the authors have no conflict of interest, and Roland Fejes Ph.D. candidate had significant contribution to the jointly published research(es). The results discussed in her thesis were not used and not intended to be used in any other qualification process for obtaining a PhD degree.

2024. 04. 24.
date

author
Dr. József Kaszaki

The publication(s) relevant to the applicant's thesis:

Tallósy, S.P., Poles, M.Z., Rutai, A. *et al.* The microbial composition of the initial insult can predict the prognosis of experimental sepsis. *Sci Rep* **11**, 22772 (2021) doi: 10.1038/s41598-021-02129-x.